

LEF-1 and TCF-1 orchestrate T_{FH} differentiation by regulating differentiation circuits upstream of the transcriptional repressor Bcl6

Youn Soo Choi^{1,6}, Jodi A Gullicksrud^{2,3,6}, Shaojun Xing², Zhouhao Zeng⁴, Qiang Shan², Fengyin Li², Paul E Love⁵, Weiqun Peng⁴, Hai-Hui Xue^{2,3} & Shane Crotty¹

Follicular helper T cells (T_{FH} cells) are specialized effector CD4⁺ T cells that help B cells develop germinal centers (GCs) and memory. However, the transcription factors that regulate the differentiation of T_{FH} cells remain incompletely understood. Here we report that selective loss of *Lef1* or *Tcf7* (which encode the transcription factor LEF-1 or TCF-1, respectively) resulted in T_{FH} cell defects, while deletion of both *Lef1* and *Tcf7* severely impaired the differentiation of T_{FH} cells and the formation of GCs. Forced expression of LEF-1 enhanced T_{FH} differentiation. LEF-1 and TCF-1 coordinated such differentiation by two general mechanisms. First, they established the responsiveness of naive CD4⁺ T cells to T_{FH} cell signals. Second, they promoted early T_{FH} differentiation via the multipronged approach of sustaining expression of the cytokine receptors IL-6R α and gp130, enhancing expression of the costimulatory receptor ICOS and promoting expression of the transcriptional repressor Bcl6.

The provision of help from T cells to B cells is a critical component of adaptive humoral immunity^{1,2}. During viral infection, the formation of germinal centers (GCs) by antigen-specific B cells requires key signals provided by follicular helper T cells (T_{FH} cells)³, which results in the development of high-affinity long-lived plasma cells and memory B cells^{4,5}. The differentiation of T_{FH} cells begins outside of B cell follicles in a stepwise fashion. Early induction of molecules key to T_{FH} differentiation, such as the transcriptional repressor Bcl6, the chemokine receptor CXCR5, the costimulatory receptor ICOS and the T cell-inhibitory receptor PD-1, occurs in the T cell zone when CD4⁺ T cells interact with antigen-presenting dendritic cells or other antigen-presenting cells, which then enable migration of the activated CD4⁺ T cells toward the border of B cell follicles. Upon recognizing cognate antigen-presenting B cells, the differentiating T_{FH} cells migrate deep inside B cell follicles and further differentiate into GC T_{FH} cells as they direct the generation of GC B cells.

The requirement for repeated interactions with antigen-presenting cells is an important feature of the differentiation of T_{FH} cells³, which is presumably connected to maintenance of the activity of critical transcription factors such as Bcl6 (refs. 6–8), Batf⁹, STAT3 (refs. 10–12), STAT1 (ref. 10) and Ascl2 (ref. 13) that support such differentiation. Among those, Bcl6 function is absolutely critical. T_{FH} differentiation is completely abrogated in *Bcl6*^{-/-} CD4⁺ T cells^{6–8}, and ectopic *Bcl6* expression in CD4⁺ T cells leads to augmented T_{FH} differentiation^{6,9}. Various signaling molecules have been identified that can regulate Bcl6 expression in CD4⁺ T cells¹⁴. However, attempts to polarize

CD4⁺ T cells to T_{FH} cells *in vitro* through the use of interleukin 6 (IL-6) and IL-21 have failed to reproducibly induce the expression of Bcl6 and CXCR5. Therefore, there are clear gaps in the understanding of the molecular requirements for Bcl6 induction and the factors that support T_{FH} differentiation³.

LEF-1 (encoded by *Lef1*) and TCF-1 (encoded by *Tcf7*) are transcription factors that contain a conserved high-mobility-group DNA-binding domain. TCF-1 and LEF-1 are known for their essential roles in early T cell development, including specification to the T cell lineage and β -selection during the CD4⁺CD8⁻ double-negative stage^{15,16}. TCF-1 and LEF-1 critically regulate commitment to the CD4⁺ T cell lineage versus commitment to the CD8⁺ T cell lineage upon completion of positive selection of CD4⁺CD8⁺ double-positive thymocytes^{17,18}. In mature CD8⁺ T cells, TCF-1 and LEF-1 regulate the generation, maturation and longevity of memory CD8⁺ T cells in response to viral or bacterial infection^{19–21}. In mature CD4⁺ T cells, TCF-1 promotes differentiation into the T_H2 subset of helper T cells *in vitro* via positive regulation of the transcription factor GATA-3 (ref. 22). TCF-1 restrains the expression of IL-17A in developing thymocytes and activated CD4⁺ T cells²³. In addition, TCF-1 can interact with the transcription factor Foxp3 and seems to oppose Foxp3-mediated repression of genes in CD4⁺ regulatory T cells²⁴.

Here we looked for undiscovered regulators of early T_{FH} differentiation and found that LEF-1 and TCF-1 were critical transcriptional regulators of such differentiation. Through the use of a knock-in reporter system and high-throughput sequencing for cDNA (RNA-seq),

¹Division of Vaccine Discovery, La Jolla Institute for Allergy and Immunology, La Jolla, California, USA. ²Department of Microbiology, University of Iowa, Iowa City, Iowa, USA. ³Interdisciplinary Immunology Graduate Program, Carver College of Medicine, University of Iowa, Iowa City, Iowa, USA. ⁴Department of Physics, The George Washington University, Washington, DC, USA. ⁵Section on Cellular and Developmental Biology, NICHD, NIH, Bethesda, Maryland, USA. ⁶These authors contributed equally to this work. Correspondence should be addressed to H.-H.X. (hai-hui-xue@uiowa.edu) or S.C. (shane@lji.org).

Received 19 March; accepted 12 June; published online 27 July 2015; doi:10.1038/ni.3226

we found that these transcription factors had high expression in T_{FH} cells after viral or bacterial infection. Deletion of *Lef1* or *Tcf7* or both in CD4⁺ T cells led to defects in T_{FH} differentiation in a dose-dependent manner. As a consequence, the magnitude of B cell responses and GC reactions was substantially diminished in mice deficient in LEF-1 and/or TCF-1, after infection. Mechanistically, LEF-1 and TCF-1 regulated multiple interacting mechanisms upstream of Bcl6 to 'preferentially' instruct activated CD4⁺ T cells to undertake T_{FH} differentiation.

RESULTS

Transcriptional profiles of early T_{FH} cells versus T_{H1} cells

The initial contact of CD4⁺ T cells with antigen-presenting cells in the T cell zone can promote the expression of key T_{FH} cell molecules, including Bcl6 and CXCR5. By 72 h into an acute viral infection, the early T_{FH} cells and T_{H1} cells have become committed to their fate^{25,26}. Early T_{FH} cells are IL-2R α ^{lo}Bcl6^{hi}Blimp1⁻CXCR5^{hi}, while early T_{H1} cells are IL-2R α ⁺ and T-bet^{hi}Bcl6⁻Blimp1^{hi} in the context of acute viral or bacterial infection^{25–28}. To identify additional factors important in the programming of T_{FH} cells, we performed gene-expression analysis of early T_{FH} cells and T_{H1} cells by RNA-seq. For this we used cells from SMARTA mice (which have transgenic expression of a T cell antigen receptor specific for the lymphocytic choriomeningitis virus (LCMV) gp61 epitope) with the additional modification of replacement of coding sequence in one allele of the endogenous gene *Prdm1* (which encodes the transcription factor Blimp1) with sequence encoding yellow fluorescent protein (Blimp1-YFP). We transferred congenically marked (CD45.1⁺) CD4⁺ T cells from those mice into

C57BL/6 (B6) (CD45.2⁺) host mice and then acutely infected the host mice with the Armstrong strain of LCMV. We isolated early T_{FH} cells and T_{H1} cells 3 d after infection and purified the cells to homogeneity by sorting IL-2R α ⁻Blimp1-YFP⁻ cells and IL-2R α ⁺Blimp1-YFP⁺ cells, respectively. We performed RNA-seq on RNA isolated from the cells and obtained transcriptome profiles of early T_{FH} cells and T_{H1} cells (Fig. 1a,b). Our analysis revealed that approximately 1,200 genes were upregulated more than 1.5-fold in early T_{FH} cells relative to their expression in T_{H1} cells, and 1,600 genes were downregulated more than 1.5-fold (Fig. 1b). Early T_{FH} cells expressed many genes that are also 'preferentially' expressed by fully differentiated T_{FH} cells and GC T_{FH} cells (*Bcl6*, *Cxcr5*, *Pdcd1*, *Pou2af1* and *Tnfsf8*, among others) and had low expression of many genes repressed in fully differentiated T_{FH} cells and GC T_{FH} cells (*Prdm1*, *Tbx21*, *Il2ra*, *Gzmb* and *Prf1*, among others) (Fig. 1a,b). Thus, major attributes of T_{FH} and T_{H1} cells were transcriptionally well defined by day 3 of an acute viral infection.

LEF-1 is a transcriptional regulator of T_{FH} differentiation

To further filter the 2,800 gene-expression differences between early T_{FH} cells and T_{H1} cells, we focused on transcription factors. We performed an additional set of RNA-seq experiments with CD4⁺ T cells activated *in vitro* under T_{H1}-polarizing conditions (IL-12 plus antibody to IL-4 (anti-IL-4) plus antibody to transforming growth factor- β) or with IL-6 (IL-6 plus antibody to interferon- γ plus anti-IL-12). We used these screening conditions because *in vitro* stimulation of CD4⁺ T cells in the presence of IL-6 resulted in some gene-expression changes associated with T_{FH} differentiation (Supplementary Fig. 1a–c). Most notably, *Il21* was robustly induced by IL-6; however,

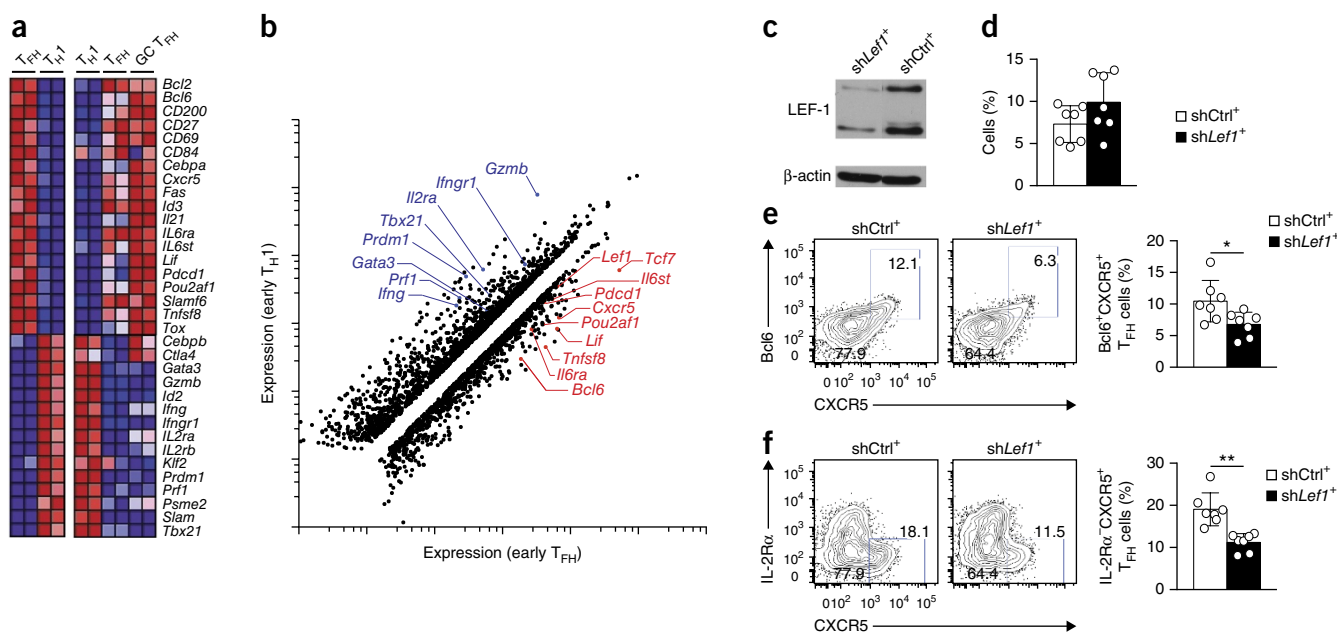


Figure 1 *Lef1* expression is associated with T_{FH} cells and LEF-1 regulates early T_{FH} differentiation. (a) RNA-seq analysis of selected genes of interest in early T_{FH} versus T_{H1} CD45.1⁺ Blimp1-YFP SMARTA cells isolated from B6 mice 3 d after transfer of SMARTA cells and infection with LCMV (left half), and of T_{H1} cells (CXCR5⁻), T_{FH} cells (PD-1^{lo}CXCR5⁺) and GC T_{FH} cells (PD-1^{hi}CXCR5⁺) sorted 8 d after LCMV from CD45.2⁺ B6 mice (right half), presented as high (red) to low (blue) expression. (b) Scatter plot of genes upregulated (red) or downregulated (blue) 1.5-fold or more in early T_{FH} cells relative to their expression in T_{H1} cells; select genes of interest are labeled. (c) Immunoblot analysis of LEF-1 (two isoforms) and β -actin (loading control) in shCtrl⁺ and shLef1⁺ SMARTA cells. (d–f) Frequency of shCtrl⁺ or shLef1⁺ CD45.1⁺ SMARTA cells (Ametrine⁺CD45.1⁺CD4⁺CD19⁻) among total CD4⁺ T cells (d) and phenotyping of shCtrl⁺ and shLef1⁺ SMARTA cells (e,f) obtained from B6 host mice 3 d after transfer of SMARTA cells infected with shRNAmir-expressing retrovirus, and infection of the hosts with LCMV. Numbers adjacent to outlined areas (e,f) indicate percent Bcl6⁺CXCR5⁺ T_{FH} cells (e) or IL-2R α ⁺CXCR5⁺ T_{FH} cells (f) among SMARTA cells. Each symbol (d–f) represents an individual mouse ($n = 7$ per group). * $P < 0.05$ and ** $P < 0.001$ (Student's t -test). Data are from one experiment with 20 mice and two biological replicates (a,b), are representative of two experiments (c) or are pooled from two independent experiments (d–f; mean \pm s.e.m.).

we did not detect major aspects of T_{FH} cell biology in IL-6-stimulated $CD4^+$ T cells, such as expression of CXCR5 protein or sustained expression of Bcl6 (refs. 3,13,29,30) (**Supplementary Fig. 1f**). This outcome suggested that key transcriptional regulators required for T_{FH} differentiation were not induced under IL-6 conditions *in vitro*. We next performed a comparative analysis of gene-expression differences between the early T_{FH} cells generated *in vivo* and the $CD4^+$ T cells stimulated *in vitro* with IL-6. To find critical previously unidentified early upstream transcriptional regulators of T_{FH} differentiation, we focused on genes that met two conditions: 'preferential' expression by early T_{FH} cells *in vivo* and lack of a difference in expression after *in vitro* stimulation with IL-6, relative to expression after stimulation without IL-6. *Lef1* satisfied these two conditions (**Fig. 1b** and **Supplementary Fig. 1d,g**), and we selected it for further analysis in part because LEF-1 is required for the formation of memory $CD8^+$ T cells²⁰ and there are similarities between the differentiation of T_{FH} cells and that of memory $CD8^+$ T cells^{25,31}.

When expressed in SMARTA $CD4^+$ T cells, a retroviral vector expressing microRNA-adapted short hairpin RNA (shRNAmir) targeting *Lef1* (*shLef1*) inhibited expression of both isoforms of LEF-1 protein (**Fig. 1c**). To determine whether the early differentiation of T_{FH} cells *in vivo* was dependent on LEF-1, we transferred SMARTA $CD45.1^+$ $CD4^+$ T cells expressing control shRNAmir (*shCtrl*) targeting *Cd19* (a gene not expressed in $CD4^+$ T cells) or *shLef1*⁺ SMARTA $CD4^+$ T cells into B6 mice. At 3 d after infection of recipient mice with LCMV, *shLef1*⁺ SMARTA $CD4^+$ T cells produced approximately half as many early T_{FH} cells as did *shCtrl*⁺ SMARTA $CD4^+$ T cells, as assessed by flow cytometry with phenotyping of either $Bcl6^+CXCR5^+$ cells (**Fig. 1e**) or $IL-2R\alpha^-CXCR5^+$ cells (**Fig. 1f**). The effect of the knockdown of LEF-1 was selective to T_{FH} differentiation, as the activation of SMARTA $CD4^+$ T cells (as assessed by upregulation of expression of the activation marker CD44; data not shown) and proliferation (**Fig. 1d**) were similar for *shCtrl*⁺ $CD4^+$ T cells and *shLef1*⁺ $CD4^+$ T cells. The reduced T_{FH}

differentiation of *shLef1*⁺ $CD4^+$ T cells indicated that LEF-1 might be an important and dose-limiting contributor to this process.

LEF-1 controls T_{FH} differentiation and GC formation

We next investigated whether LEF-1 function in $CD4^+$ T cells was important for GC T_{FH} differentiation and GC reactions. We transferred *shLef1*⁺ or *shCtrl*⁺ SMARTA $CD4^+$ T cells into B6 mice and analyzed the recipient mice 8 d after acute infection with LCMV. The activation and proliferation of $CD4^+$ T cells were not affected by reduced *Lef1* expression, compared with that of *shCtrl*⁺ $CD4^+$ T cells (**Fig. 2a**), but the T_{FH} differentiation of *shLef1*⁺ cells was impaired (**Fig. 2b,c**). The T_{FH} -differentiation defect of *shLef1*⁺ cells was less severe at day 8 than that observed on day 3 (**Fig. 2b**), potentially due to the fact that sustained gene knockdown in $CD4^+$ T cells *in vivo* is difficult to accomplish under conditions of rapid proliferation. We observed milder T_{FH} -differentiation defects for most retrovirus-expressed shRNAmirs, including shRNAmir directed against *Bcl6*, at peak proliferation time points than at early time points after infection (data not shown). Nevertheless, *shLef1*⁺ SMARTA $CD4^+$ T cells showed defective differentiation into GC T_{FH} cells, identified here as $PSGL-1^loCXCR5^+$ T cells (**Fig. 2d**) or $Bcl6^+CXCR5^+$ T cells (**Fig. 2e**), compared with such differentiation of *shCtrl*⁺ SMARTA $CD4^+$ T cells. As a result, the development of GC B cells ($Bcl6^+CD19^+$) was moderately impaired in the presence of *shLef1*⁺ SMARTA $CD4^+$ T cells relative to their development in the presence of *shCtrl*⁺ cells (**Fig. 2f**). Thus, a reduction in LEF-1 expression in $CD4^+$ T cells resulted in a loss of T_{FH} cells and GC T_{FH} cells and a proportional loss of GC B cells during an immune response to LCMV.

Ablation of *Lef1* diminishes GC T_{FH} differentiation

We next investigated the role of LEF-1 in T_{FH} differentiation through the use of mice with conditional deletion of *Lef1*. Lineage-specific deletion of loxP-flanked *Lef1* alleles (*Lef1^{fl/fl}*) in thymocytes through the use of Cre recombinase expressed from the T cell-specific *Cd4*

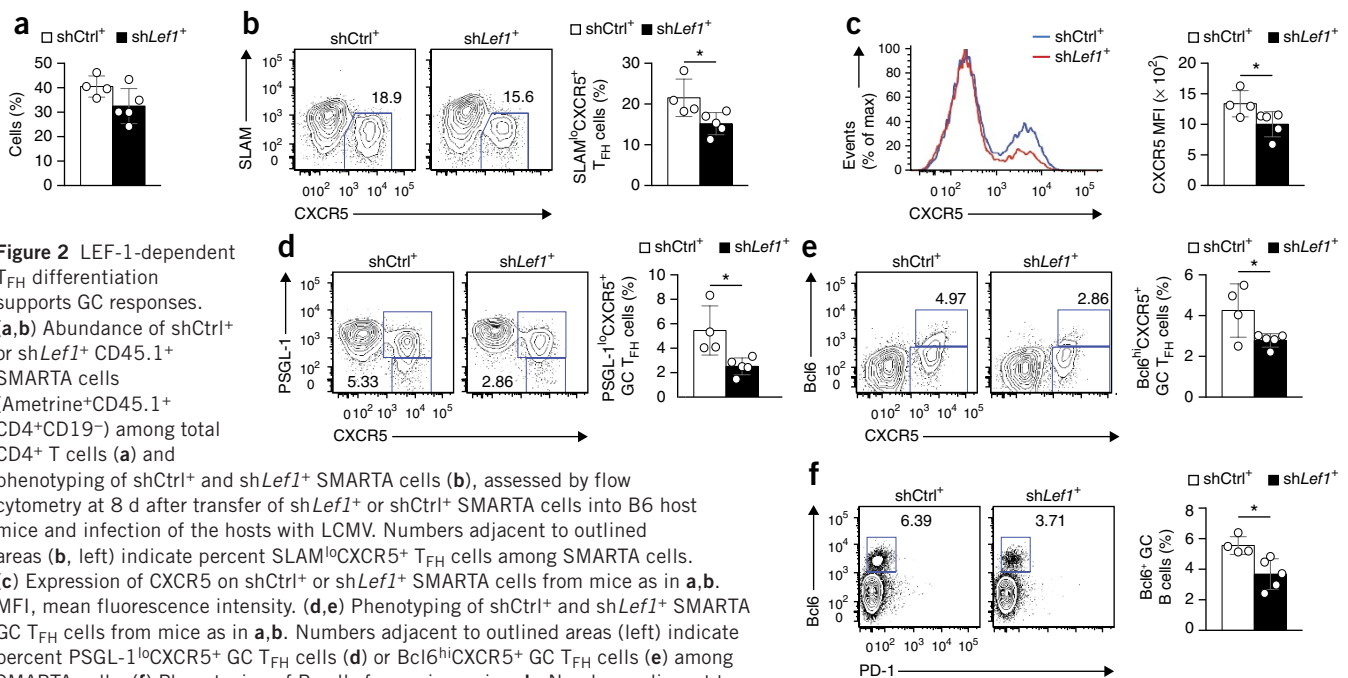


Figure 2 LEF-1-dependent T_{FH} differentiation supports GC responses. (**a,b**) Abundance of *shCtrl*⁺ or *shLef1*⁺ $CD45.1^+$ SMARTA cells (Ametrine⁺ $CD45.1^+$ $CD4^+CD19^-$) among total $CD4^+$ T cells (**a**) and phenotyping of *shCtrl*⁺ and *shLef1*⁺ SMARTA cells (**b**), assessed by flow cytometry at 8 d after transfer of *shLef1*⁺ or *shCtrl*⁺ SMARTA cells into B6 host mice and infection of the hosts with LCMV. Numbers adjacent to outlined areas (**b**, left) indicate percent $SLAMF6^loCXCR5^+$ T_{FH} cells among SMARTA cells. (**c**) Expression of CXCR5 on *shCtrl*⁺ or *shLef1*⁺ SMARTA cells from mice as in **a,b**. MFI, mean fluorescence intensity. (**d,e**) Phenotyping of *shCtrl*⁺ and *shLef1*⁺ SMARTA GC T_{FH} cells from mice as in **a,b**. Numbers adjacent to outlined areas (left) indicate percent $PSGL-1^loCXCR5^+$ GC T_{FH} cells (**d**) or $Bcl6^+CXCR5^+$ GC T_{FH} cells (**e**) among SMARTA cells. (**f**) Phenotyping of B cells from mice as in **a,b**. Numbers adjacent to outlined areas (left) indicate percent $Bcl6^+CD19^+$ GC B cells among total B cells. Each symbol represents an individual mouse ($n = 4-5$ per group). * $P < 0.05$ (Student's *t*-test). Data are representative of two independent experiments (mean \pm s.e.m.).

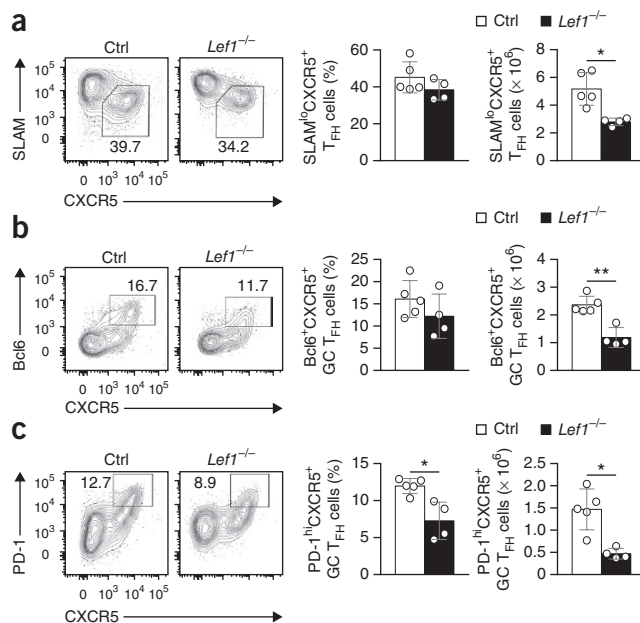
Figure 3 Genetic ablation of LEF-1 impairs GC T_{FH} differentiation.

Flow cytometry of cells from the spleen of *Lef1*^{-/-} mice and their control littermates (Ctrl) 8 d after infection with vaccinia virus. Numbers adjacent to outlined areas (left) indicate percent SLAM^{hi}CXCR5⁺ T_{FH} cells (a), Bcl6⁺CXCR5⁺ GC T_{FH} cells (b) or PD-1^{hi}CXCR5⁺ GC T_{FH} cells (c) among cells gated as CD44^{hi}CD62L^{lo}GFP⁺CD4⁺ T cells. Each symbol represents an individual mouse. **P* < 0.01 and ***P* < 0.001 (Student's *t*-test). Data are pooled from four independent experiments (mean ± s.d.).

promoter (*Cd4*-Cre) impairs CD4⁺ T cell lineage 'choice' and diminishes the output of CD4⁺ T cells¹⁸. To avoid this, we used mice with transgenic expression of Cre driven by the promoter of the human gene encoding the activation-costimulation molecule CD2 (*hCD2*-Cre), which results in gene ablation in mature T cells³². We also crossed mice to mice expressing an allele for the expression of green fluorescent protein (GFP) from the ubiquitously expressed 'Rosa26' locus (*Rosa26*-STOP-GFP; called '*Rosa26*^{GFP}' here). As marked by GFP expression due to excision of the *loxP*-flanked transcription-translation 'stop' sequence from the *Rosa26*^{GFP} allele, over 70% of splenic CD4⁺ T cells in *Rosa26*^{GFP}*hCD2*-Cre⁺ mice were GFP⁺, whereas less than 15% of CD4⁺ thymocytes were GFP⁺ (Supplementary Fig. 2a). We crossed *Rosa26*^{GFP}*hCD2*-Cre⁺ mice to the *Lef1*^{fl/fl} strain to generate *Rosa26*^{GFP}*Lef1*^{fl/fl}*hCD2*-Cre⁺ mice (called '*Lef1*^{-/-} mice' here). Both isoforms of LEF-1 were completely ablated in GFP⁺ CD4⁺ T cells from *Lef1*^{-/-} mice (Supplementary Fig. 2b). Late deletion of LEF-1 did not detectably affect thymocyte development or cause aberrant activation of mature T cells (Supplementary Fig. 2d,f,h,i) but reduced total thymic cellularity by approximately 15% and mature CD4⁺ T cells by approximately 25% (Supplementary Fig. 2e,g). To determine the effect of LEF-1 deficiency in CD4⁺ T cells on T_{FH} differentiation, we infected *Lef1*^{-/-} mice and their control littermates (*Lef1*^{+/fl}*hCD2*-Cre⁻ or *Lef1*^{+/fl}*hCD2*-Cre⁺) with vaccinia virus and assessed the presence of CD44^{hi}CD62L⁻ activated GFP⁺ CD4⁺ splenic T cells on day 8 after infection. The frequency of T_H1 cells (SLAM^{hi}CXCR5⁻) was similar in *Lef1*^{-/-} mice and their control littermates, although the absolute number of SLAM^{hi}CXCR5⁻ T_H1 cells was modestly lower in *Lef1*^{-/-} mice than in their control littermates (*P* = 0.51; Supplementary Fig. 3), consistent with the slightly smaller CD4⁺ T cell compartment in uninfected *Lef1*^{-/-} mice than in their uninfected control littermates (Supplementary Fig. 2g). In contrast, the number of SLAM^{hi}CXCR5⁺ T_{FH} cells was more markedly diminished in vaccinia virus-infected *Lef1*^{-/-} mice compared with the number of these cells in their infected control littermates (Fig. 3a). In particular, the number of GC T_{FH} cells was considerably lower in *Lef1*^{-/-} mice than in their control littermates (by Bcl6⁺CXCR5⁺ and PD-1^{hi}CXCR5⁺ phenotyping; Fig. 3b,c). These data further supported the proposal of role for LEF-1 in directing the differentiation of T_{FH} cells.

TCF-1 expression is retained in T_{FH} cells but not in T_H1 cells

RNA-seq analysis of early T_{FH} cells and T_H1 cells isolated from B6 mice revealed that *Tcf7* also had high expression in early T_{FH} cells, but *Tcf7* was not induced by *in vitro* stimulation of CD4⁺ T cells with IL-6 (Fig. 1b and Supplementary Fig. 1e,g). Given that LEF-1 and TCF-1 are related transcription factors, we investigated whether TCF-1 was also an early regulator of T_{FH} differentiation. For this purpose, we generated mice with sequence encoding GFP inserted into the *Tcf7* locus (*Tcf7*^{GFP}; Supplementary Fig. 4a). The *Tcf7*-GFP reporter had abundant expression in CD4⁺ T cells, CD8⁺ T cells and CD4⁺CD25⁺ regulatory T cells but was absent in B220⁺ cells (Supplementary Fig. 4b-d), which demonstrated the reporter fidelity. The expression of *Tcf7*-GFP was highest in CD44^{lo}CD62L⁺ naive T cells but

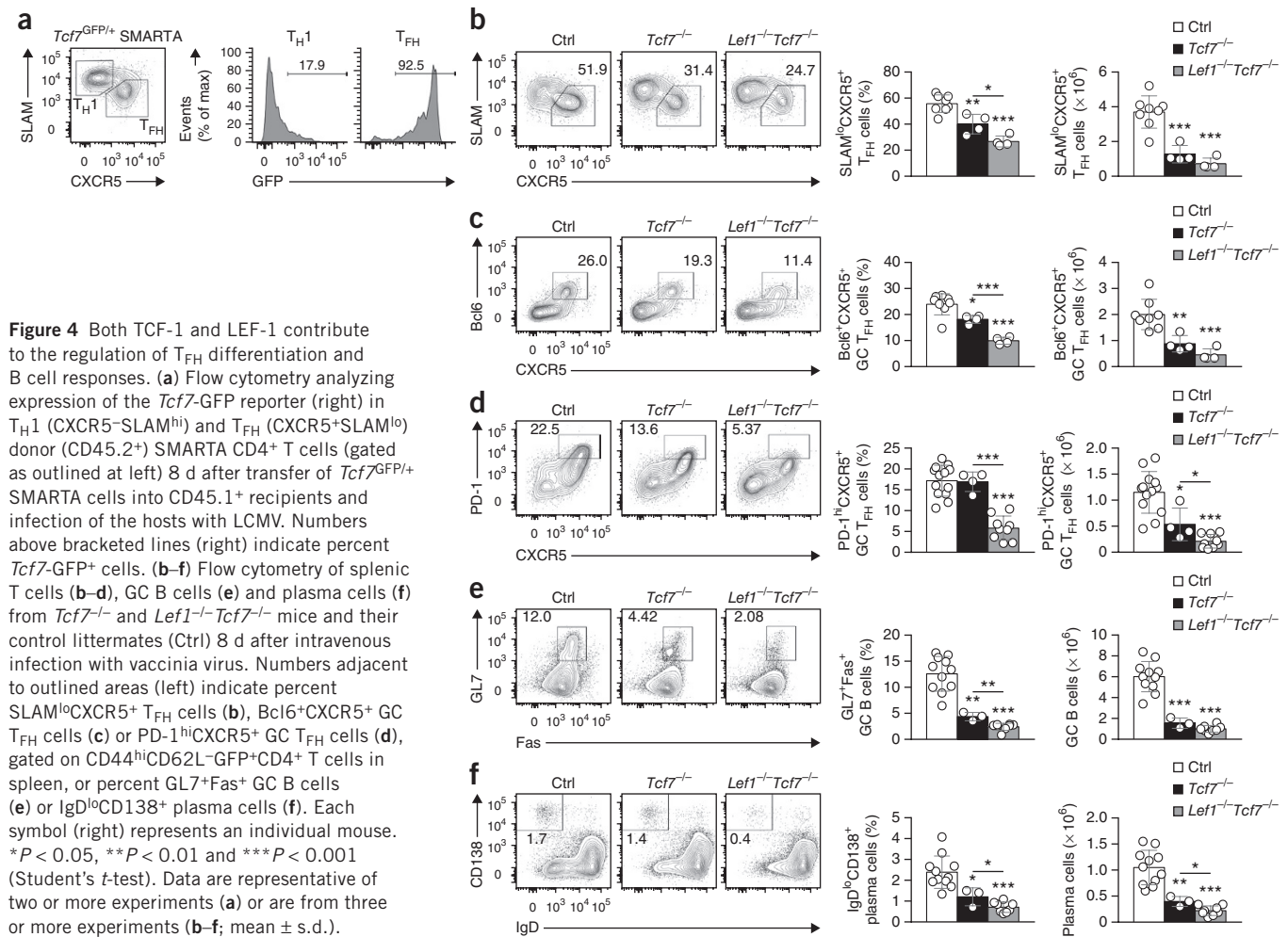


was moderately diminished in antigen-experienced T cell subsets such as CD44^{hi}CD62L⁺ memory-phenotype T cells, and particularly CD44^{hi}CD62L⁻ effector-phenotype T cells (Supplementary Fig. 4b,c). To analyze TCF-1 expression kinetics in antigen-specific CD4⁺ T cells, we generated *Tcf7*^{GFP/+} SMARTA mice and adoptively transferred naive CD44^{lo}CD62L⁺ CD45.2⁺ CD4⁺ T cells from those mice into CD45.1⁺ congenic recipients. Following infection with LCMV, *Tcf7*-GFP expression was greatly diminished in SLAM^{hi}CXCR5⁻ T_H1 cells relative to its expression in naive CD4 T cells by day 8 after infection, while *Tcf7*-GFP expression was maintained at a high level by most SLAM^{lo}CXCR5⁺ T_{FH} cells (Fig. 4a).

We next investigated whether the retention of TCF-1 expression was associated with the T_{FH}-differentiation program in response to other *in vivo* stimuli. Following adoptive transfer of *Tcf7*^{GFP} SMARTA CD4⁺ T cells, we infected recipient mice with *Listeria monocytogenes* expressing the gp61 epitope of LCMV. In other experiments, we directly infected *Tcf7*^{GFP/+} mice with vaccinia virus, as a second viral infection model. Whereas SLAM^{hi}CXCR5⁻ T_H1 cells that developed in both systems downregulated *Tcf7*-GFP expression, SLAM^{lo}CXCR5⁺ T_{FH} cells generated in response to both the bacterial and viral infections retained high expression of *Tcf7*-GFP (Supplementary Fig. 4e,f). Given that TCF-1 is known to be markedly downregulated in effector CD8⁺ T cells³³, these observations indicated that retention of TCF-1 expression at the effector phase of a T cell response was unique to T_{FH} cells and further suggested a possible requirement for TCF-1 in T_{FH} differentiation.

Both LEF-1 and TCF-1 are essential for T_{FH} cell responses

To address the role of TCF-1 in T_{FH} cells, we generated *Rosa26*^{GFP}*Tcf7*^{fl/fl}*hCD2*-Cre⁺ mice (called '*Tcf7*^{-/-} mice' here), in which all isoforms of TCF-1 were ablated in GFP⁺ CD4⁺ T cells (Supplementary Fig. 2c). To investigate the functional redundancy between LEF-1 and TCF-1, we also crossed *Tcf7*^{-/-} with *Lef1*^{-/-} mice to generate *Lef1*^{-/-}*Tcf7*^{-/-} mice (*Rosa26*^{GFP}*Lef1*^{fl/fl}*Tcf7*^{fl/fl}*hCD2*-Cre⁺). Similar to *Lef1*^{-/-} mice, *Tcf7*^{-/-} mice and *Lef1*^{-/-}*Tcf7*^{-/-} mice did not have T cell-development defects or aberrant activation of mature T cells in (Supplementary Fig. 2). Although we observed slightly less thymic



and splenic cellularity in *Tcf7*^{-/-} mice than in their control littermates (*Lef1*^{+/+}*Tcf7*^{+/+}hCD2-Cre⁻ or *Lef1*^{+/+}*Tcf7*^{+/+}hCD2-Cre⁺), this difference was not evident in *Tcf7*^{-/-} or *Lef1*^{-/-}*Tcf7*^{-/-} mice (Supplementary Fig. 2d,f,h,i). We assessed the CD4⁺ T cell responses of *Lef1*^{-/-}*Tcf7*^{-/-} mice in response to infection with vaccinia virus. On day 8 after infection, analysis of CD44^{hi}CD62L⁻ activated GFP⁺ CD4⁺ T cells revealed that the frequency and number of SLAMF6^{lo}CXCR5⁺ T_{FH} cells were diminished in *Tcf7*^{-/-} mice compared with that of control mice (Fig. 4b), with a comparable reduction in GC T_{FH} cells (Bcl6⁺CXCR5⁺ and PD-1^{hi}CXCR5⁺ phenotyping; Fig. 4c,d). We found greater defects in *Lef1*^{-/-}*Tcf7*^{-/-} mice than in *Tcf7*^{-/-} mice (Fig. 4b–d), which indicated that both LEF-1 and TCF-1 contributed to regulating the differentiation of T_{FH} cells.

Consistent with the observations reported above, *Tcf7*^{-/-} and *Lef1*^{-/-}*Tcf7*^{-/-} mice exhibited a significantly lower frequency and number of GL7⁺Fas⁺ GC B cells than that of control mice (Fig. 4e), with the most severe GC B cell defect in *Lef1*^{-/-}*Tcf7*^{-/-} mice (Fig. 4e). The number of IgD^{lo}CD138⁺ plasma cells was moderately reduced in *Tcf7*^{-/-} mice but was severely compromised in *Lef1*^{-/-}*Tcf7*^{-/-} mice, relative to that in their control littermates (Fig. 4f). As a result, the production of vaccinia virus-specific antibodies was significantly impaired in *Lef1*^{-/-}*Tcf7*^{-/-} mice compared with that of their control littermates (*P* = 0.017; Supplementary Fig. 5). In summary, our data indicated critical roles for LEF-1 and TCF-1 in T_{FH} differentiation and, consequently, B cell-helping functions, in a CD4⁺ T cell-intrinsic manner.

Ectopic *Lef1* expression augments T_{FH} differentiation

We next investigated whether enhanced expression of one of these transcription factors (LEF-1 and TCF-1) could augment the T_{FH} differentiation of antigen-specific CD4⁺ T cells. Given that LEF-1 and TCF-1 exhibited overlapping activities in instructing the differentiation of T_{FH} cells, we assessed the T_{FH} differentiation of CD4⁺ T cells after ectopic expression of LEF-1. LEF-1 can be expressed as two isoforms in CD4⁺ T cells due to differential promoter use (Fig. 1c), with the full-length isoform containing an amino-terminal β -catenin-binding domain. We constructed a retrovirus expressing full-length *Lef1* (*Lef1*-RV) and confirmed increased expression of LEF-1 in *Lef1*-RV⁺ SMARTA CD45.1⁺ CD4⁺ T cells by flow cytometry (Fig. 5a) and immunoblot analysis (data not shown). We infected CD45.1⁺ SMARTA CD4⁺ T cells with control retrovirus expressing GFP alone (GFP-RV) or *Lef1*-RV and transferred the cells into B6 mice, which we then infected with LCMV. The overall activation and proliferation of *Lef1*-RV⁺ CD4⁺ T cells was normal compared with that of GFP-RV⁺ CD4⁺ T cells (Fig. 5b and data not shown). Ectopic LEF-1 expression resulted in enhanced T_{FH} development of *Lef1*-RV⁺ cells relative to that of GFP-RV⁺ cells at 8 d after infection (Fig. 5c). Moreover, we found that *Lef1*-RV⁺ T_{H1} cells (SLAMF6^{hi}CXCR5⁻) unexpectedly exhibited higher expression of the canonical T_{FH} molecules CXCR5 (Fig. 5d) and PD-1 (Fig. 5e) than that of their GFP-RV⁺ counterparts. Most notably, GC T_{FH} cells (with a phenotype of either PSGL-1^{lo}CXCR5⁺ or PD-1^{hi}CXCR5⁺) developed at a significantly higher frequency among *Lef1*-RV⁺ SMARTA CD4⁺ T cells than among their GFP-RV⁺ counterparts (Fig. 5f,g).

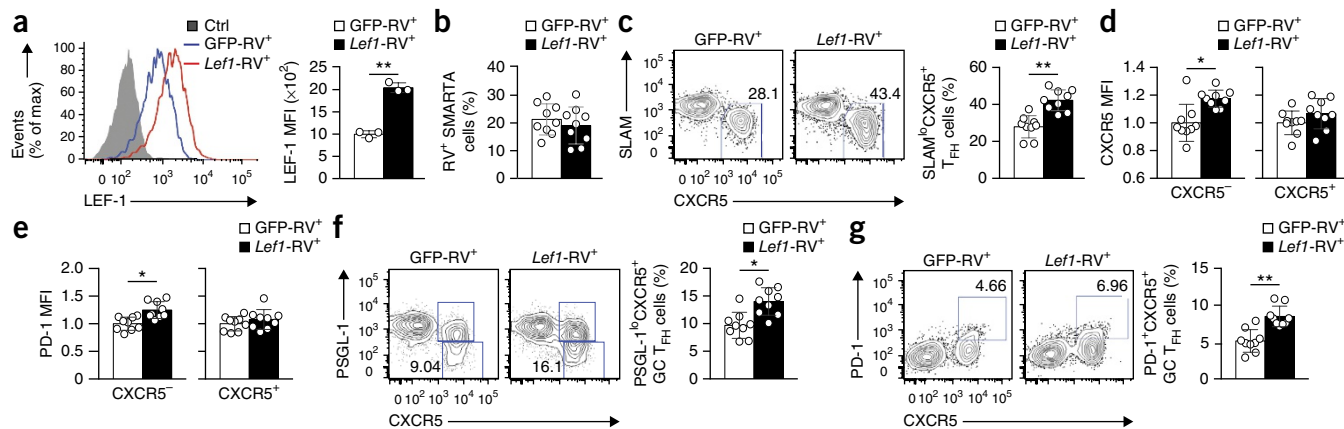


Figure 5 Enhanced *Lef1* expression leads to augmented T_{FH} differentiation. (a) Flow cytometry analyzing the expression of LEF-1 in GFP-RV⁺ and *Lef1*-RV⁺ SMARTA cells. Ctrl, isotype-matched control antibody. (b) Frequency of GFP-RV⁺ or *Lef1*-RV⁺ (RV⁺) SMARTA cells (GFP⁺CD45.1⁺CD4⁺CD19⁻) among total CD4⁺ T cells, assessed by flow cytometry at 8 d after transfer of SMARTA cells into B6 mice (CD45.2⁺) and infection of the hosts with LCMV. (c) Phenotype of GFP-RV⁺ or *Lef1*-RV⁺ SMARTA cells as in b. Numbers adjacent to outlined areas (left) indicate percent SLAMF6⁺CXCR5⁺ T_{FH} cells among GFP-RV⁺ or *Lef1*-RV⁺ SMARTA cells. (d, e) Expression of the canonical T_{FH} cell markers CXCR5 (d) and PD-1 (e) on CXCR5⁻ T_{FH} cells and CXCR5⁺ T_{FH} cells among GFP-RV⁺ and *Lef1*-RV⁺ cells as in b, normalized to the mean fluorescence intensity of GFP-RV⁺ cells in each group. (f, g) Phenotype of GC T_{FH} cells from mice as in b. Numbers adjacent to outlined areas (left) indicate percent PSGL-1⁺CXCR5⁺ GC T_{FH} cells (f) or PD-1^{hi}CXCR5⁺ GC T_{FH} cells (g) among GFP-RV⁺ or *Lef1*-RV⁺ SMARTA cells. Each symbol represents an individual mouse ($n = 9$ per group). * $P < 0.01$ and ** $P < 0.001$ (Student's *t*-test). Data are pooled from two independent experiments (mean \pm s.e.m.).

LEF-1 enhances expression of IL-6 receptors and ICOS

To gain insight into how LEF-1 regulates T_{FH} differentiation, we performed RNA-seq analysis of GFP-RV⁺ or *Lef1*-RV⁺ CXCR5^{lo} T_{H1} and CXCR5^{hi} T_{FH} SMARTA CD4⁺ T cells. We next used the transcriptional signatures of T_{FH} and GC T_{FH} cells and gene-set-enrichment analysis (GSEA) to investigate whether *Lef1*-RV⁺ T_{H1} cells showed enrichment for expression of these gene signatures compared with their expression in control (GFP-RV⁺) T_{H1} cells. We found substantial enrichment for expression of the T_{FH} cell and GC T_{FH} cell gene signatures (Supplementary Table 1) in T_{H1} cells constitutively expressing *Lef1* (normalized enrichment score, 1.21 (T_{FH} cells) or 1.29 (GC T_{FH} cells); Fig. 6a) compared with their expression in control T_{H1} cells. Detailed examination revealed that the expression of *Il6ra*, *Il6st*, *Bcl6*, *Cxcr5*, *Slamf6* and *Pou2af1* was particularly different in *Lef1*-RV⁺ T_{H1} cells than in GFP-RV⁺ T_{H1} cells (Fig. 6b).

Given the induction of both *Il6ra* and *Il6st* (which encode the IL-6R α and gp130 receptors for IL-6, respectively) in *Lef1*-RV⁺ T_{H1} cells and the fact that signaling via IL-6 receptors is one of the earliest signals that instruct T_{FH} differentiation³, we investigated whether LEF-1-augmented T_{FH} differentiation might be mediated through enhanced surface expression of IL-6R α and gp130. We analyzed the expression of IL-6R α and gp130 on the surface of *Lef1*-RV⁺ or GFP-RV⁺ SMARTA CD4⁺ T cells at day 3 after infection with LCMV, a time when signaling via IL-6 receptors is known to be critical for T_{FH} differentiation¹⁰. The ectopic expression of LEF-1 in *Lef1*-RV⁺ SMARTA CD4⁺ T cells resulted in higher expression of IL-6R α than that on GFP-RV⁺ SMARTA CD4⁺ T cells (Fig. 6c). In a comparison of IL-6R α expression on naive CD4⁺ T cells and that on activated *Lef1*-RV⁺ or GFP-RV⁺ SMARTA CD4⁺ T cells, we found that overexpression LEF-1 reduced the downregulation of IL-6R α expression observed on activated GFP-RV⁺ CD4⁺ T cells (Fig. 6c). Overexpression of LEF-1 had a similar effect on gp130, reducing the downregulation of gp130 expression observed on activated GFP-RV⁺ CD4⁺ T cells (Fig. 6d). We then assessed the expression of IL-6R α and gp130 on T_{FH} and T_{H1} subpopulations. We observed modestly higher IL-6R α expression on T_{FH} cells, whereas *Lef1*-RV⁺ T_{H1} cells expressed >150% more IL-6R α than did GFP-RV⁺ T_{H1} cells (Fig. 6e). While the expression of gp130

was only moderately higher on total *Lef1*-RV⁺ SMARTA CD4⁺ T cells than on GFP-RV⁺ SMARTA CD4⁺ T cells (Fig. 6d), gp130 expression was 'preferentially' upregulated on *Lef1*-RV⁺ T_{H1} cells compared with its expression on GFP-RV⁺ T_{H1} cells (Fig. 6f).

RNA-seq analysis also revealed that *Icos* expression was upregulated in *Lef1*-RV⁺ T_{H1} cells compared with its expression in GFP-RV⁺ T_{H1} cells (Fig. 6b). Because ICOS has essential roles during both early stages and late stages of T_{FH} differentiation²⁶, we further assessed ICOS expression. Expression of ICOS protein was higher on *Lef1*-RV⁺ T cells than on GFP-RV⁺ cells (Fig. 6g), and its upregulation occurred predominantly on *Lef1*-RV⁺ T_{H1} cells (Fig. 6h), to levels comparable to those on GFP-RV⁺ T_{FH} cells. These observations indicated that LEF-1 functioned to help CD4⁺ T cells retain surface expression of IL-6 receptors and upregulate ICOS expression to enhance the responsiveness of activated CD4⁺ T cells to signaling via IL-6 and the ligand for ICOS, two essential signals for early T_{FH} differentiation.

We then investigated whether overexpression of LEF-1 could restore T_{FH} differentiation in the absence of *Bcl6*. *Bcl6*^{fl/fl}*Cd4*-Cre CD4⁺ T cells fail to differentiate into T_{FH} cells during acute viral infection or immunization with protein³⁴. *Lef1*-RV⁺ or GFP-RV⁺ *Bcl6*^{fl/fl}*Cd4*-Cre SMARTA CD4⁺ T cells transferred into B6 mice failed to differentiate into T_{FH} cells *in vivo* at day 8 after infection of the recipient mice with LCMV (Supplementary Fig. 6). These results indicated that LEF-1-mediated regulation of the IL-6 receptor complex and ICOS expression acted upstream of *Bcl6* expression early in T_{FH} differentiation.

Extensive gene-regulation defects in *Lef1*^{-/-}*Tcf7*^{-/-} GC T_{FH} cells

We further assessed the requirements for LEF-1 and TCF-1 in the expression of key T_{FH} cell molecules by transcriptomic analysis of *Lef1*^{-/-}*Tcf7*^{-/-} GC T_{FH} cells. We performed RNA-seq analysis of total RNA extracted from GC T_{FH} cells (sorted as PD-1^{hi}CXCR5⁺ cells among CD44^{hi}CD62L^{lo}GFP⁺CD4⁺ T cells) isolated from *Lef1*^{-/-}*Tcf7*^{-/-} and control mice (*Lef1*^{+/+}*Tcf7*^{+/+}*hCD2*-Cre⁻ or *Lef1*^{+/+}*Tcf7*^{+/+}*hCD2*-Cre⁺) on day 8 after infection with vaccinia virus. We found that 306 genes were downregulated and 668 genes were upregulated in *Lef1*^{-/-}*Tcf7*^{-/-} GC T_{FH} cells relative to their expression in control GC T_{FH} cells (false-discovery rate, <0.01; change in

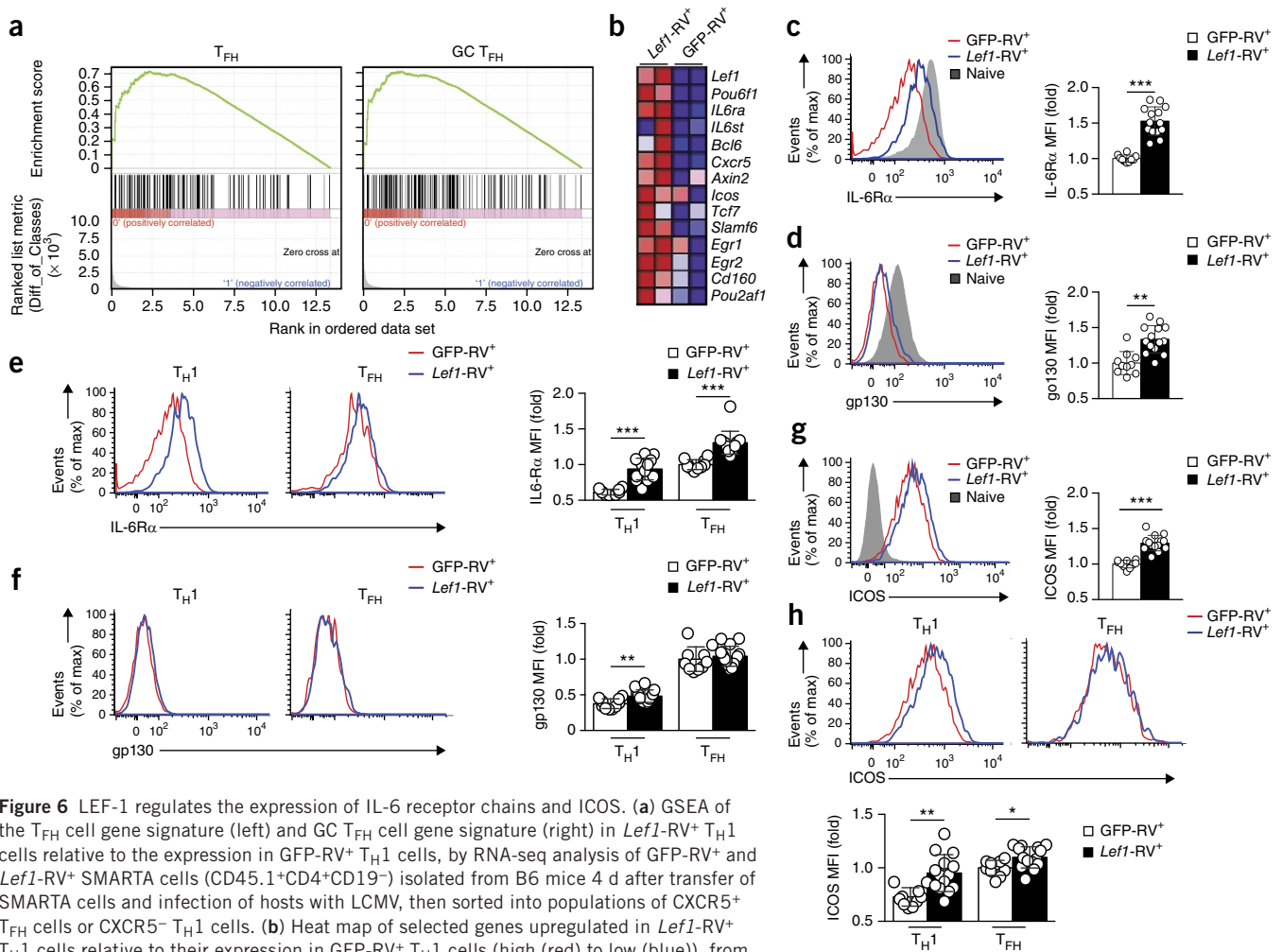
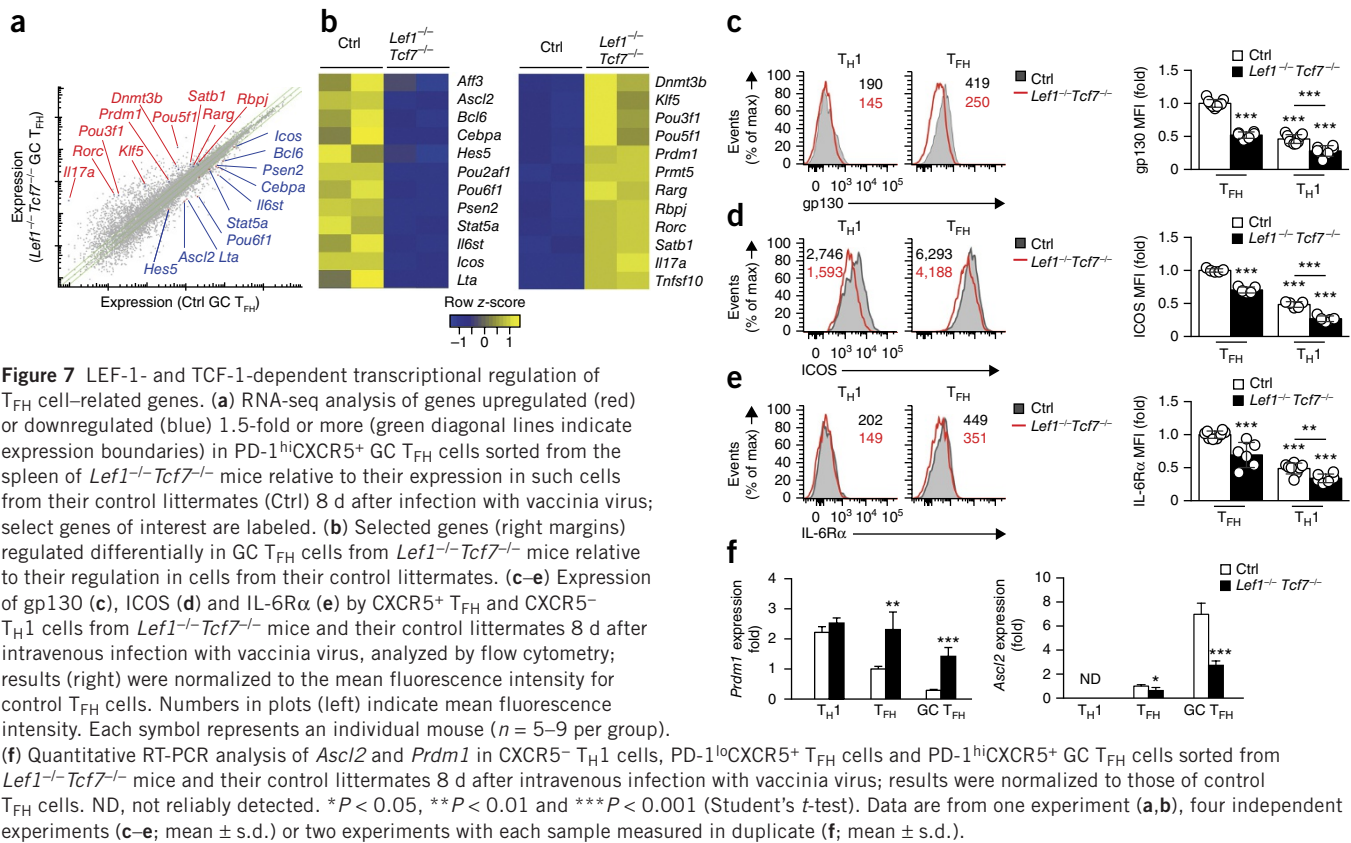


Figure 6 LEF-1 regulates the expression of IL-6 receptor chains and ICOS. **(a)** GSEA of the T_{FH} cell gene signature (left) and GC T_{FH} cell gene signature (right) in $Lef1$ -RV+ T_{FH} cells relative to the expression in GFP-RV+ T_{H1} cells, by RNA-seq analysis of GFP-RV+ and $Lef1$ -RV+ SMARTA cells (CD45.1⁺CD4⁺CD19⁻) isolated from B6 mice 4 d after transfer of SMARTA cells and infection of hosts with LCMV, then sorted into populations of CXCR5⁺ T_{FH} cells or CXCR5⁻ T_{H1} cells. **(b)** Heat map of selected genes upregulated in $Lef1$ -RV+ T_{FH} cells relative to their expression in GFP-RV+ T_{H1} cells (high (red) to low (blue)), from mice as in **a**. **(c, d)** Expression of IL-6R α (**c**) and gp130 (**d**) on GFP-RV+ or $Lef1$ -RV+ SMARTA cells (CD45.1⁺CD4⁺CD19⁻), assessed by flow cytometry 3 d after transfer of SMARTA cells into B6 host mice (CD45.2⁺) and infection of the hosts with LCMV. **(e, f)** Expression of IL-6R α (**e**) and gp130 (**f**) on GFP-RV+ or $Lef1$ -RV+ T_{H1} and T_{FH} cells from mice as in **c, d**. **(g, h)** Expression of ICOS on total RV+ SMARTA cells (**g**) or on the CXCR5⁺ T_{FH} and CXCR5⁻ T_{H1} cell subpopulations (**h**) from mice as in **c, d**. Each symbol (**c–h**) represents an individual mouse ($n = 10–14$ per group). * $P < 0.05$, ** $P < 0.01$ and *** $P < 0.001$ (Student's t -test). Data are from one experiment with eight mice in each and two biological replicates (**a, b**) or are pooled from three experiments (**c–h**; mean \pm s.e.m.).

expression, ≥ 1.5 -fold; **Fig. 7a**). In line with the enhanced expression of *Il6st* and *Icos* induced by overexpression of LEF-1, $Lef1$ ^{-/-}*Tcf7*^{-/-} GC T_{FH} cells had a much lower abundance of *Il6st* and *Icos* transcripts than did control cells (**Fig. 7b**). Flow cytometry showed lower expression of gp130 and ICOS on $Lef1$ ^{-/-}*Tcf7*^{-/-} CXCR5⁺ T_{FH} cells than on control T_{FH} cells (**Fig. 7c, d**). Although the decrease in *Il6ra* mRNA in $Lef1$ ^{-/-}*Tcf7*^{-/-} GC T_{FH} cells did not reach statistical significance in the transcriptomic analysis, expression of IL-6R α protein was consistently lower on $Lef1$ ^{-/-}*Tcf7*^{-/-} CXCR5⁺ T_{FH} cells than on control T_{FH} cells (**Fig. 7e**). These observations indicated essential and overlapping roles for both LEF-1 and TCF-1 in supporting the expression of IL-6 receptors and ICOS during T_{FH} differentiation.

The abundance of *Bcl6* transcripts was lower in PD-1^{hi}CXCR5⁺ GC T_{FH} cells from $Lef1$ ^{-/-}*Tcf7*^{-/-} mice than in those from control mice, while the expression of *Prdm1* was substantially elevated in $Lef1$ ^{-/-}*Tcf7*^{-/-} GC T_{FH} cells (**Fig. 7b**). *Bcl6* and *Blimp1* are known to have mutually antagonistic roles during T_{FH} differentiation⁶. *Blimp1* directly inhibits *Bcl6* expression and is a potent inhibitor of T_{FH} differentiation^{6,28,30}. We confirmed the enhanced expression of *Prdm1* in $Lef1$ ^{-/-}*Tcf7*^{-/-} PD-1^{hi}CXCR5⁺ GC T_{FH} by quantitative PCR (**Fig. 7f**).

This increase was specific to GC T_{FH} cells (PD-1^{hi}CXCR5⁺) and T_{FH} cells (PD-1^{lo}CXCR5⁺), because T_{H1} cells (CXCR5⁻) from $Lef1$ ^{-/-}*Tcf7*^{-/-} mice and control mice had similar expression of *Prdm1* (**Fig. 7f**). The transcription factor *Ascl2* is important in T_{FH} differentiation¹³. *Ascl2* expression was lower in $Lef1$ ^{-/-}*Tcf7*^{-/-} GC T_{FH} cells than in control cells, but this reduction was less pronounced in PD-1^{lo}CXCR5⁺ T_{FH} cells (**Fig. 7f**). Expression of *Rorc* (which encodes the transcription factor ROR γ t) and *Il17a* was almost completely absent in control GC T_{FH} cells, but these genes were expressed in $Lef1$ ^{-/-}*Tcf7*^{-/-} GC T_{FH} cells (**Fig. 7b**). Although the expression of genes characteristic of T_{H17} cells is not normally observed after infection with vaccinia virus, our observations were in line with the known role of TCF-1 in restraining T_{H17} differentiation²³ and indicated that LEF-1 and TCF-1 might suppress alternative helper T cell fates during T_{FH} differentiation, perhaps in conjunction with *Bcl6*, which is also known to suppress alternative cell fates³. Other transcriptional changes observed in $Lef1$ ^{-/-}*Tcf7*^{-/-} GC T_{FH} cells compared with the transcription in control GC T_{FH} cells included differential expression of genes encoding transcription factors of the POU family (decreased expression of *Pou2af1* and *Pou6f1*, and increased expression of *Pou3f1* and



Pou5f1) and key molecules of the Notch signaling pathway (decreased expression of *Hes5* and *Psen2*, and increased expression of *Rbpj*) (Fig. 7b). The role of these factors in T_{FH} cells remains to be investigated. Overall, these observations suggested that LEF-1 and TCF-1 contributed to the regulation of many genes in activated, antigen-specific $CD4^+$ T cells *in vivo*, including the positive regulation of *Bcl6* and repression of *Blimp1* to induce T_{FH} differentiation.

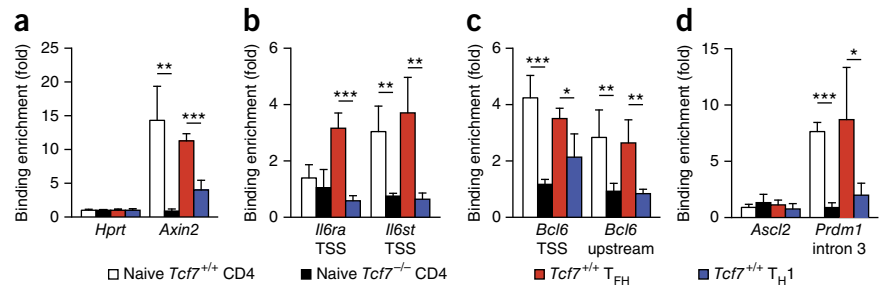
Direct binding of TCF-1 to key T_{FH} cell-associated genes

We used chromatin immunoprecipitation (ChIP) followed by deep sequencing (ChIP-seq) to determine whether LEF-1 and TCF-1 directly regulated the differentially expressed genes identified above. Both TCF-1 and LEF-1 have a highly homologous high-mobility-group DNA-binding domain that recognizes the same DNA consensus motif. Because reagents used for ChIP analysis of TCF-1 are of substantially higher quality than those available for such analysis of LEF-1, we focused on identifying TCF-1-bound genes in T_{FH} cells. Because most T_{FH} cells retained TCF-1 expression similar to that of naive $CD4^+$ T cells (Fig. 4a), we used our ChIP-seq data for TCF-1 that we obtained with naive wild-type $CD4^+$ T cells (data not shown) as a reference for the identification of potential DNA-binding sites for TCF-1. We observed enrichment for binding of TCF-1 at the transcription start site (TSS) of *Il6st*, the TSS of *Bcl6*, a region 2.8 kilobases upstream of the *Bcl6* TSS (-2.8 kb) and intron 3 of *Prdm1* in naive $CD4^+$ T cells, relative to its binding in the majority of the genome, but it was not associated with *Il6ra* or *Ascl2* (Supplementary Fig. 7a). We then performed ChIP analysis of TCF-1 in wild-type and *Tcf7*^{-/-} naive $CD4^+$ T cells to ensure binding specificity. As a positive control, TCF-1 bound to the TSS of *Axin2*, a well-characterized TCF-1-responsive gene¹⁵, in wild-type naive $CD4^+$ T cells, and this binding was completely abrogated in *Tcf7*^{-/-} naive $CD4^+$ T cells (Fig. 8a). In addition, T_{FH} cells

($CXCR5^+$) from B6 mice infected with vaccinia virus showed enrichment for the binding of TCF-1 to *Axin2* relative to its binding in T_{H1} cells ($CXCR5^-$) from such mice (Fig. 8a), consistent with higher expression of TCF-1 protein in T_{FH} cells than in T_{H1} cells. TCF-1 bound to *Il6st* in wild-type naive $CD4^+$ T cells (Fig. 8b, right), and T_{FH} cells also showed enrichment for such binding relative to binding in the *Tcf7*^{-/-} negative control cells (Fig. 8b). Although TCF-1 did not bind to *Il6ra* in wild-type naive $CD4^+$ T cells, it was recruited to the *Il6ra* TSS in wild-type T_{FH} cells (Fig. 8b, left), which suggested that recruitment of TCF-1 to this site is part of the T_{FH} differentiation program. Wild-type T_{H1} cells did not exhibit enrichment for the binding of TCF-1 at *Il6st* or *Il6ra* compared with its binding in naive $CD4^+$ T cells (Fig. 8b), in line with the diminished expression of both *Il6Rα* and *gp130* on T_{H1} cells (Fig. 7c,e). We did not detect binding of TCF-1 to the TSS of *Icos* (Supplementary Fig. 7b). These data suggested that TCF-1 directly regulated induction of the expression of IL-6 receptor chains to sustain expression of the IL-6 receptor complex by activated $CD4^+$ T cells *in vivo*, which allowed T_{FH} differentiation (Supplementary Fig. 8).

We next investigated by ChIP the association of TCF-1 with genes encoding transcription factors key to T_{FH} differentiation. TCF-1 bound to intron 3 of *Prdm1*, the major regulatory site of *Prdm1* expression³⁵, in both naive $CD4^+$ T cells and $CXCR5^+$ T_{FH} cells (Fig. 8d), which suggested direct involvement of TCF-1 and its homolog LEF-1 in the suppression of *Blimp1* in T_{FH} cells. Given that *Prdm1* is not expressed by naive $CD4^+$ T cells, binding of TCF-1 at this site suggested that TCF-1 might antagonize *Prdm1* expression upon T cell activation. In addition, we observed specific binding of TCF-1 to the TSS of *Bcl6* and an upstream regulatory region of *Bcl6* in naive $CD4^+$ T cells (Fig. 8c), and this binding pattern was maintained in T_{FH} cells (Fig. 8c). We observed robust enrichment for TCF-1 at *Prdm1*, *Bcl6*, *Il6ra* and

Figure 8 TCF-1 binds to key T_{FH} cell-associated genes in T_{FH} cells. ChIP analysis of the binding of TCF-1 to the positive control gene *Axin2* (a), the TSS of *Il6ra* and *Il6st* (b), the TSS and a regulatory region 2.8 kb upstream of *Bcl6* (c), and the TSS of *Ascl2* and intron 3 of *Prdm1* (d) in naive *Tcf7*^{+/+} CD4⁺ T cells (CD44^{lo}CD62L⁺), naive *Tcf7*^{-/-} CD4⁺ T cells (GFP⁺CD44^{lo}CD62L⁺CD4⁺), *Tcf7*^{+/+} T_{FH} cells (CXCR5⁺CD44^{hi}CD62L⁻CD4⁺) and *Tcf7*^{+/+} T_{H1} cells (CXCR5⁻CD44^{hi}CD62L⁻CD4⁺), with the last two populations sorted from B6 mice 8 d after infection with vaccinia virus; results were normalized to those obtained by ChIP with immunoglobulin G and are presented relative to those obtained for the promoter region of the control gene *Hprt*. * $P < 0.05$, ** $P < 0.01$ and *** $P < 0.001$ (Student's *t*-test). Data are from three independent experiments (mean and s.d.).



Il6st in wild-type T_{FH} cells relative to its abundance at those genes in *Tcf7*^{-/-} T_{FH} cells (Supplementary Fig. 7b). We did not observe enrichment for TCF-1 binding in the *Ascl2* TSS (Fig. 8c,d), although we could not exclude the possibility that *Ascl2* is regulated by LEF-1 and TCF-1 through more distal regulatory regions. Binding of TCF-1 to the upstream region of *Bcl6* and the *Prdm1* intron was abrogated in T_{H1} cells relative to its binding in T_{FH} cells (Fig. 8d), in line with the substantially reduced expression of TCF-1 in T_{H1} cells. These observations suggested that downregulation of TCF-1 in T_{H1} cells was important for upregulation of Blimp1 and Blimp1-mediated repression of *Bcl6* in T_{H1} cells, while retention of TCF-1 in early T_{FH} cells ensured proper upregulation of *Bcl6* and subsequent suppression of Blimp1 during T_{FH} differentiation (Supplementary Fig. 8).

DISCUSSION

T_{FH} differentiation can be initiated at an early time point during T cell activation, but the regulators of this important 'decision' process are still being defined. Here we initiated an investigation to identify previously unknown pathways in T_{FH} differentiation by characterizing genes differentially expressed in early T_{FH} cells *in vivo* relative to their expression in T_{H1} cells but not modulated by supplementation with IL-6 *in vitro*. We found that a pair of transcription factors, LEF-1 and TCF-1, influenced T_{FH} differentiation by regulating circuits upstream of *Bcl6*. We found that LEF-1 and TCF-1 coordinated T_{FH} differentiation by two general mechanisms. First, they established the responsiveness of naive CD4⁺ T cells to T_{FH} cell signals by promoting the expression of IL-6 receptor chains and binding to *Prdm1* and *Bcl6*. Second, they promoted early T_{FH} differentiation of activated CD4⁺ T cells via multipronged activities that sustained expression of IL-6R α and gp130, enhanced ICOS expression and promoted *Bcl6* expression while inhibiting Blimp1 expression.

IL-6 is a critical early regulator of T_{FH} differentiation, as *Il6*^{-/-} mice fail to undergo any differentiation of T_{FH} cells during the dendritic cell-priming phase of an acute antiviral immune response¹⁰. In mice whose dendritic cells constitutively overexpress IL-6, the main alteration in phenotype observed is a substantial increase in T_{FH} cells and GCs³⁶. Therefore, regulation of the expression of IL-6 receptors on naive CD4⁺ T cells and early activated CD4⁺ T cells is a mechanism by which LEF-1 and TCF-1 influence T_{FH} differentiation.

Bcl6 is essential for T_{FH} differentiation, while Blimp1 is a powerful antagonist of such differentiation. Our observations that expression of LEF-1 resulted in aberrant expression of *Bcl6* in T_{H1} cells, Blimp1 expression was aberrantly upregulated in *Lef1*^{-/-}*Tcf7*^{-/-} GC T_{FH} cells, and the genes encoding *Bcl6* and Blimp1 were both targets directly bound by TCF-1 indicated that LEF-1 and TCF-1 probably dually regulate both of these critical transcription factors. While we cannot rule out the possibility that the de-repression of *Prdm1* resulted from

reduced *Bcl6* expression in *Lef1*^{-/-}*Tcf7*^{-/-} T_{FH} and GC T_{FH} cells, we speculate that LEF-1 and TCF-1 directly repress *Prdm1* expression. LEF-1 and TCF-1 are known to positively and negatively regulate gene expression, depending on the interacting factors. For examples, both proteins can interact with the coactivator β -catenin and with transcriptional corepressors of the TLE family, and LEF-1 and TCF-1 repress *Cd4* in CD8⁺ T cells¹⁸. Future analysis of molecular mechanisms by which LEF-1 and TCF-1 regulate *Prdm1* and *Bcl6* will be important, as will analysis of how LEF-1 and TCF-1 interact with other regulators of *Bcl6* and *Prdm1*, such as STAT1, STAT3, STAT5, Foxo1 and Klf2 (refs. 3,10,11,28,37,38). Nevertheless, our data have provided proof that LEF-1 and TCF-1 regulate the balance between *Bcl6* expression and Blimp1 expression.

ICOS expression was selectively impaired on *Lef1*^{-/-}*Tcf7*^{-/-} T_{FH} cells, and ICOS expression was enhanced on *Lef1*-RV⁺ cells. In multiple models, moderate changes in ICOS have been observed to enhance the differentiation of T_{FH} cells³⁸⁻⁴¹ or their function⁴². ICOS seems to be not a direct target of LEF-1 and TCF-1, although distal *cis* elements have not been explored. Alternatively, ICOS might be indirectly regulated by LEF-1 and TCF-1. Future studies should further elucidate the LEF-1 and TCF-1 signaling axes that modulate ICOS expression. Overall, the combined influence of LEF-1 and TCF-1 on IL-6R α , gp130, *Bcl6*, Blimp1 and ICOS produces a dense network of interactions that create a strong pro- T_{FH} cell signaling environment in a cell that sustains the expression of LEF-1 and/or TCF-1.

The functions of LEF-1 and TCF-1 probably continue to be important in fully differentiated T_{FH} cells and GC T_{FH} cells. LEF-1 and TCF-1 both continue to be expressed in GC T_{FH} cells. *Bcl6* expression is essential in GC T_{FH} cells³, and continued regulation of both *Bcl6* and *Prdm1* are central aspects of GC T_{FH} cell biology. ICOS is also a major regulator of GC T_{FH} cell biology^{26,40}. Signaling via the IL-6 receptor is not usually essential in GC T_{FH} cells due to compensatory abilities of IL-21 or IL-27 at later time points^{29,43,44}. Nevertheless, the IL-6 receptor probably has a major role in sustaining GC T_{FH} cells under normal physiological conditions. IL-6 is required for sustaining T_{FH} cell and GC responses during chronic infection with LCMV in mice⁴⁵, and IL-6 is positively associated with T_{FH} cells and GCs in macaques positive for simian immunodeficiency virus⁴⁶.

The activities of LEF-1 and TCF-1 seem to pre-program the responsiveness of a given naive CD4⁺ T cell to T_{FH} cell signals, prior to any exposure of the cell to antigen. Therefore, we speculate that transient or sustained inflammatory or pathogenic conditions that alter the expression of LEF-1 or TCF-1 in naive T cells might have a global effect that alters the capacity of naive CD4⁺ T cells to respond to T_{FH} cell-induction signals in the presence of pathogens or autoimmunity triggers. Ultimately, it will be useful to determine how homeostatic signals act in concert with LEF-1 and TCF-1 to modulate the

expression or poised status of T_{FH} cell-associated genes in naive CD4⁺ T cells to properly orchestrate the development progression from naive cell to the T_{FH} cell or non-T_{FH} cell fate.

LEF-1 and TCF-1 have high expression in resting naive CD4⁺ and CD8⁺ T cells, but the expression of LEF-1 and TCF-1 is downregulated in effector CD8⁺ T cells and T_{H1} cells, which suggests *Lef1* and *Tcf7* are regulated by T cell activation. Dwell time at the T cell antigen receptor influences T_{FH} differentiation versus non-T_{FH} differentiation in a manner intrinsic to the signal strength of the receptor⁴⁷. We speculate these processes may be interrelated.

In conclusion, our study has identified previously unknown roles for LEF-1 and TCF-1 in T_{FH} differentiation. Better understanding of the downstream targets of LEF-1 and TCF-1 in activated CD4⁺ T cells will improve the understanding of T_{FH} cell biology. Finally, better understanding of the signals that regulate LEF-1 and TCF-1 will have implications for understanding how to enhance or inhibit the differentiation of T_{FH} cells.

METHODS

Methods and any associated references are available in the [online version of the paper](#).

Accession codes. GEO: RNA-seq data, [GSE66781](#) and [GSE67336](#).

Note: Any Supplementary Information and Source Data files are available in the online version of the paper.

ACKNOWLEDGMENTS

We thank J. Yang for help with *ex vivo* screening of target genes obtained from RNA-seq analysis of early T_{FH} cells and T_{H1} cells; Z. Fu for help with GSEA and for the generation of heat maps; the La Jolla Institute Flow Cytometry Flow Cytometry Core Facility (C. Kim, K.V. Gunst and L. Nosworthy) and the University of Iowa Flow Cytometry Core facility (J. Fishbaugh, H. Vignes and G. Rasmussen) for cell sorting; T. Takemori (RIKEN, Research Center for Integrated Medical Sciences) for *Bcl6*^{fl/fl} mice; I. Antoshechkin (Millard and Muriel Jacobs Genetics and Genomics Laboratory at the Caltech) for *Tcf7*^{-/-}*Lef1*^{-/-} RNA-seq; and J.T. Harty (University of Iowa) for vaccinia virus (for the Xue laboratory). Supported by the American Cancer Society (RSG-11-161-01-MPC to H.-H.X.), the US National Institutes of Health (AI105351, AI112579, AI115149 and AI119160 to H.-H.X.; AI113806 to W.P.; AI109976, AI063107 and AI072543 to S.C.; and AI007485 for support for to J.A.G.) and the University of Iowa Presidential Graduate Research Fellowship program (J.A.G.).

AUTHOR CONTRIBUTIONS

Y.S.C., J.A.G., S.X., Q.S. and F.L. performed the experiments and analyzed the data; Z.Z. analyzed the RNA-seq data under the supervision of W.P.; P.E.L. provided reagents; Y.S.C., H.-H.X. and S.C. conceived of the project and wrote the paper; and H.-H.X. and S.C. supervised the overall study.

COMPETING FINANCIAL INTERESTS

The authors declare no competing financial interests.

Reprints and permissions information is available online at <http://www.nature.com/reprints/index.html>.

- Crotty, S. A brief history of T cell help to B cells. *Nat. Rev. Immunol.* **15**, 185–189 (2015).
- Ueno, H., Banachereau, J. & Vinuesa, C.G. Pathophysiology of T follicular helper cells in humans and mice. *Nat. Immunol.* **16**, 142–152 (2015).
- Crotty, S. T follicular helper cell differentiation, function, and roles in disease. *Immunity* **41**, 529–542 (2014).
- Shlomchik, M.J. & Weisel, F. Germinal center selection and the development of memory B and plasma cells. *Immunity. Rev.* **247**, 52–63 (2012).
- Victoria, G.D. & Nussenzweig, M.C. Germinal centers. *Annu. Rev. Immunol.* **30**, 429–457 (2012).
- Johnston, R.J. *et al.* Bcl6 and Blimp-1 are reciprocal and antagonistic regulators of T follicular helper cell differentiation. *Science* **325**, 1006–1010 (2009).
- Nurieva, R.I. *et al.* Bcl6 mediates the development of T follicular helper cells. *Science* **325**, 1001–1005 (2009).

- Yu, D. *et al.* The transcriptional repressor Bcl-6 directs T follicular helper cell lineage commitment. *Immunity* **31**, 457–468 (2009).
- Ise, W. *et al.* The transcription factor BATF controls the global regulators of class-switch recombination in both B cells and T cells. *Nat. Immunol.* **12**, 536–543 (2011).
- Choi, Y.S., Eto, D., Yang, J.A., Lao, C. & Crotty, S. Cutting edge: STAT1 is required for IL-6-mediated Bcl6 induction for early follicular helper cell differentiation. *J. Immunol.* **190**, 3049–3053 (2013).
- Nurieva, R.I. *et al.* Generation of T follicular helper cells is mediated by interleukin-21 but independent of T helper 1, 2, or 17 cell lineages. *Immunity* **29**, 138–149 (2008).
- Ray, J.P. *et al.* Transcription factor STAT3 and type I interferons are corepressive insulators for differentiation of follicular helper and T helper 1 cells. *Immunity* **40**, 367–377 (2014).
- Liu, X. *et al.* Transcription factor achaete-scute homologue 2 initiates follicular T-helper-cell development. *Nature* **507**, 513–518 (2014).
- Choi, Y.S., Yang, J.A. & Crotty, S. Dynamic regulation of Bcl6 in follicular helper CD4 T (T_{fh}) cells. *Curr. Opin. Immunol.* **25**, 366–372 (2013).
- Weber, B.N. *et al.* A critical role for TCF-1 in T-lineage specification and differentiation. *Nature* **476**, 63–68 (2011).
- Yu, S. *et al.* The TCF-1 and LEF-1 transcription factors have cooperative and opposing roles in T cell development and malignancy. *Immunity* **37**, 813–826 (2012).
- Steinke, F.C. & Xue, H.-H. From inception to output, Tcf1 and Lef1 safeguard development of T cells and innate immune cells. *Immunity. Res.* **59**, 45–55 (2014).
- Steinke, F.C. *et al.* TCF-1 and LEF-1 act upstream of Th-POK to promote the CD4+ T cell fate and interact with Runx3 to silence *Cd4* in CD8+ T cells. *Nat. Immunol.* **15**, 646–656 (2014).
- Jeannet, G. *et al.* Essential role of the Wnt pathway effector Tcf-1 for the establishment of functional CD8 T cell memory. *Proc. Natl. Acad. Sci. USA* **107**, 9777–9782 (2010).
- Zhou, X. & Xue, H.-H. Cutting edge: generation of memory precursors and functional memory CD8+ T cells depends on T cell factor-1 and lymphoid enhancer-binding factor-1. *J. Immunol.* **189**, 2722–2726 (2012).
- Zhou, X. *et al.* Differentiation and persistence of memory CD8+ T cells depend on T cell factor 1. *Immunity* **33**, 229–240 (2010).
- Yu, Q. *et al.* T cell factor 1 initiates the T helper type 2 fate by inducing the transcription factor GATA-3 and repressing interferon- γ . *Nat. Immunol.* **10**, 992–999 (2009).
- Yu, Q., Sharma, A., Ghosh, A. & Sen, J.M. T cell factor-1 negatively regulates expression of IL-17 family of cytokines and protects mice from experimental autoimmune encephalomyelitis. *J. Immunol.* **186**, 3946–3952 (2011).
- van Loosdregt, J. *et al.* Canonical Wnt signaling negatively modulates regulatory T cell function. *Immunity* **39**, 298–310 (2013).
- Choi, Y.S. *et al.* Bcl6 expressing follicular helper CD4 T cells are fate committed early and have the capacity to form memory. *J. Immunol.* **190**, 4014–4026 (2013).
- Choi, Y.S. *et al.* ICOS receptor instructs T follicular helper cell versus effector cell differentiation via induction of the transcriptional repressor Bcl6. *Immunity* **34**, 932–946 (2011).
- Pepper, M., Pagán, A.J., Igyártó, B.Z., Taylor, J.J. & Jenkins, M.K. Opposing signals from the bcl6 transcription factor and the interleukin-2 receptor generate T helper 1 central and effector memory cells. *Immunity* **35**, 583–595 (2011).
- Johnston, R.J., Choi, Y.S., Diamond, J.A., Yang, J.A. & Crotty, S. STAT5 is a potent negative regulator of TFH cell differentiation. *J. Exp. Med.* **209**, 243–250 (2012).
- Eto, D. *et al.* IL-21 and IL-6 are critical for different aspects of B cell immunity and redundantly induce optimal follicular helper CD4 T cell (T_{fh}) differentiation. *PLoS ONE* **6**, e17739 (2011).
- Oestreich, K.J., Mohn, S.E. & Weinmann, A.S. Molecular mechanisms that control the expression and activity of Bcl-6 in T_{H1} cells to regulate flexibility with a T_{FH}-like gene profile. *Nat. Immunol.* **13**, 405–411 (2012).
- Chen, R. *et al.* In vivo RNA interference screens identify regulators of antiviral CD4+ and CD8+ T cell differentiation. *Immunity* **41**, 325–338 (2014).
- Vacchio, M.S. *et al.* A ThPOK-LRF transcriptional node maintains the integrity and effector potential of post-thymic CD4+ T cells. *Nat. Immunol.* **15**, 947–956 (2014).
- Zhao, D.-M. *et al.* Constitutive activation of Wnt signaling favors generation of memory CD8 T cells. *J. Immunol.* **184**, 1191–1199 (2010).
- Nance, J.P., Belanger, S., Johnston, R.J., Takemori, T. & Crotty, S. Cutting edge: T follicular helper cell differentiation is defective in the absence of Bcl6 BTB repressor domain function. *J. Immunol.* **194**, 5599–5603 (2015).
- Tunayaplin, C. *et al.* Direct repression of *prdm1* by Bcl-6 inhibits plasmacytic differentiation. *J. Immunol.* **173**, 1158–1165 (2004).
- Kim, S.J., Zou, Y.R., Goldstein, J., Reizis, B. & Diamond, B. Tolerogenic function of Blimp-1 in dendritic cells. *J. Exp. Med.* **208**, 2193–2199 (2011).
- Lee, J.-Y. *et al.* The transcription factor KLF2 restrains CD4+ T follicular helper cell differentiation. *Immunity* **42**, 252–264 (2015).
- Stone, E.L. *et al.* ICOS coreceptor signaling inactivates the transcription factor FOXO1 to promote T_{fh} cell differentiation. *Immunity* **42**, 239–251 (2015).
- Pratama, A. *et al.* MicroRNA-146a regulates ICOS-ICOSL signalling to limit accumulation of T follicular helper cells and germinal centres. *Nat. Commun.* **6**, 6436 (2015).

40. Weber, J.P. *et al.* ICOS maintains the T follicular helper cell phenotype by down-regulating Krüppel-like factor 2. *J. Exp. Med.* **212**, 217–233 (2015).
41. Vogel, K.U. *et al.* Roquin paralogs 1 and 2 redundantly repress the Icos and Ox40 costimulator mRNAs and control follicular helper T cell differentiation. *Immunity* **38**, 655–668 (2013).
42. Xu, H. *et al.* Follicular T-helper cell recruitment governed by bystander B cells and ICOS-driven motility. *Nature* **496**, 523–527 (2013).
43. Batten, M. *et al.* IL-27 supports germinal center function by enhancing IL-21 production and the function of T follicular helper cells. *J. Exp. Med.* **207**, 2895–2906 (2010).
44. Poholek, A.C. *et al.* In vivo regulation of Bcl6 and T follicular helper cell development. *J. Immunol.* **185**, 313–326 (2010).
45. Harker, J.A., Lewis, G.M., Mack, L. & Zuniga, E.I. Late interleukin-6 escalates T follicular helper cell responses and controls a chronic viral infection. *Science* **334**, 825–829 (2011).
46. Petrovas, C. *et al.* CD4 T follicular helper cell dynamics during SIV infection. *J. Clin. Invest.* **122**, 3281–3294 (2012).
47. Tubo, N.J. *et al.* Single naive CD4+ T cells from a diverse repertoire produce different effector cell types during infection. *Cell* **153**, 785–796 (2013).

ONLINE METHODS

Mice and viral infection. C57BL/6J (B6), B6.SJL, *Cd4-Cre*, and *Rosa26^{GFP}* mice were from the Jackson Laboratory. Mouse strains described below were from in-house breeders of either the La Jolla Institute or the University of Iowa animal facility. SMARTA mice (specific for LCMV glycoprotein amino acids 66–77 presented by I-Ab)⁴⁸ and *Tcf7^{fl/fl}* and *Lef1^{fl/fl}* mice^{16,18} have been described. *Bcl6^{fl/fl}* mice were from T. Takemori⁴⁹ and *hCD2-Cre* mice were from P.E.L.³². Blimp1-YFP mice (expressing a bacterial artificial chromosome transgene) were crossed to the SMARTA strain to generate Blimp1-YFP SMARTA mice²⁶. *Tcf7-GFP* reporter mice were generated in-house (unpublished data). All mice analyzed were 6–12 weeks of age, and both sexes were included without randomization or ‘blinding’ of researchers to mouse or sample identity. All mouse experiments were performed under protocols approved by the Institutional Animal Use and Care Committees of the La Jolla Institute and the University of Iowa. For acute viral infection, 2.5×10^5 to 5.0×10^5 plaque-forming units of LCMV (Armstrong strain) and 2.5×10^5 plaque-forming units of vaccinia virus were used. Virus was prepared in plain DMEM and was injected intraperitoneally or intravenously.

Flow cytometry. Single-cell suspensions were prepared from the spleen of mice infected with LCMV or vaccinia virus, and surfaces were stained as described^{16,26}. The fluorochrome-conjugated antibodies were as follows: anti-CD4 (RM4-5), anti-CD44 (IM7), anti-CD62L (MEL-14), anti-PD-1 (J43), anti-IL-6R α (D7715A7), anti-gp130 (KGP130), anti-ICOS (C398.4A), anti-Fas (15A7), anti-GL7 (GL7), anti-IgD (11-26), anti-CD138 (281-2) and anti-Bcl6 (K112-91) (all from eBiosciences); anti-SLAM (TC15-12F12.2; BioLegend); and anti-PSGL-1 (2PH1; BD Biosciences). For detection of CXCR5, a two-step²⁶ or three-step⁶ staining protocol was used with biotinylated anti-CXCR5 or unconjugated anti-CXCR5, respectively (2G8; BD Biosciences). For intracellular detection of Bcl6, surface-stained cells were fixed and permeabilized with the Foxp3/Transcription Factor Staining Buffer Set (eBiosciences), followed by incubation with fluorochrome-conjugated anti-Bcl6. Data were collected on an LSRII and a FACSVerse (BD Biosciences) and were analyzed with FlowJo software (TreeStar).

Immunoblot analysis. For analysis of the knockdown of LEF-1 or targeted deletion of TCF-1 and LEF-1, shCtrl⁺ and shLef1⁺ SMARTA cells or CD4⁺ and CD8⁺ T cells (5×10^5 each) were sorted, followed by denaturation for 5 min at 100 °C in SDS loading buffer. Cell lysates were probed with anti-TCF-1 (C46C7; Cell Signaling Technology), anti-LEF-1 (C18A7 and C12A5; Cell Signaling Technology) or anti- β -actin (loading control; I-19; Santa Cruz Biotechnology).

Retroviral transduction. Naive SMARTA CD4⁺ T cells were purified by negative selection with either magnetic beads (Miltenyi Biotec) or an EasySep kit (StemCell), and were resuspended in D-10 medium (DMEM containing 10% FCS, 2 mM GlutaMax (Life Technologies), 100 U/ml penicillin and streptomycin (Life Technologies) and 50 μ M β -mercaptoethanol) with 2 ng/ml human IL-7 or 10 ng/ml human IL-2 (Peprotech). 2×10^6 SMARTA cells were seeded in 24-well plates coated with 8 μ g/ml anti-CD3 (17A2; BioXcell) and anti-CD28 (37.51; BioXcell). Retroviral supernatants were added at 24 and 36 h after stimulation. After 72 h of *in vitro* stimulation, SMARTA cells were transferred into six-well plates in D-10 medium with 10 ng/ml human IL-2, followed by incubation for 2 d. One day before reporter-expressing cells were sorted (with a FACSAria from BD Biosciences) for transfer, the culture medium was replaced with D-10 medium with 2 ng/ml human IL-7. Detailed information has been published⁵⁰.

Cell sorting. All cell sorting was done on a FACSAria (BD Biosciences). For RNA-seq analysis, early T_{FH} cells (IL-2R α -Blimp1-YFP⁻) or early T_{H1} cells (IL-2R α -Blimp1-YFP⁺) among SMARTA cells, or the CXCR5⁻ subset (T_{H1}), PD-1^{lo}CXCR5⁺ subset (T_{FH}), and PD-1^{hi}CXCR5⁺ subset (GC T_{FH}) of activated GFP⁺CD4⁺ splenic T cells of *Lef1^{-/-}Tcf7^{-/-}* mice or their control littermates were sorted on day 3 after infection with LCMV or on day 8 after infection with vaccinia virus, respectively. GFP-RV⁺ or *Lef1-RV⁺* SMARTA cells were sorted as SLAM^{hi}CXCR5^{lo} (T_{H1}) or SLAM^{lo}CXCR5^{hi} (T_{FH}) cells on day 4 after LCMV infection. For ChIP analysis, CXCR5⁻ (T_{H1}) and CXCR5⁺ (T_{FH}) cells

were sorted from activated CD4⁺ splenic T cells on day 8 after infection with vaccinia virus. Also, CD44^{lo}CD62L^{hi} naive CD4⁺ T cells were sorted from wild-type or *Tcf7^{-/-}* (*Tcf7^{fl/fl}Cd4-Cre*) mice.

Retrovirus production and cell transfer. Mouse *Lef1* cDNA (6401514; Open Biosystems) was cloned into a retroviral expression vector (pMIG-GFP). The *Lef1*-specific shRNA sequence (Transomic) was cloned into pLMPd-Ametrine vector, as reported^{26,31}. The vector pLMPd-Ametrine with shRNA sequence (5'-TGCTGTTGACAGTGAGCGAATGGATAAGTCTGACGACCT ATAGTGAAGCCACAGATGTATAGGTCGTCAGACTTATCCATGTGCCTA ATGCCTCGGA-3') directed against mouse *Cd19* served as a negative control (shCtrl) in knockdown experiments. Virions were obtained from Plat-E cells as described⁵⁰. Culture supernatants were collected 24 and 48 h after transfection, then were filtered through a 0.45- μ m syringe filter and saved at 4 °C until used for transduction.

Naive or retrovirus-transduced SMARTA cells were transferred intravenously into mice via the retro-orbital sinus. For transduced SMARTA cells, 100% of the transferred cells were transduced (Ametrine⁺CD45.1⁺). The number of cells transferred was 4×10^5 to 5×10^5 , 2×10^5 , or 5×10^3 SMARTA cells on day 3, 4 or 8, respectively.

In vitro activation of CD4⁺ T cells. Naive SMARTA cells were negatively isolated through the use of a CD4⁺ T cell isolation kit (Miltenyi or StemCell). 2×10^6 SMARTA cells were seeded on 24-well plates coated with 8 μ g/ml anti-CD3 (17A2; BioXcell) and anti-CD28 (37.51; BioXcell). For T_{H1} polarization, SMARTA cells were treated with 20 μ g/ml of anti-IL-4 (11B11; BioXcell) and antibody to transforming growth factor- β (1D11; BioXcell) and 20 ng/ml of recombinant mouse IL-12 (Peprotech). For IL-6 condition, 10 μ g/ml of antibody to interferon IFN- γ (XMG1.2; BioXcell) and anti-IL-12 (R1-5D9; BioXcell) and 20 ng/ml of recombinant mouse IL-6 (Peprotech) were added to the culture medium.

Quantitative RT-PCR. Total RNA from the sorted cells was extracted and reverse-transcribed, and quantitative PCR was performed as described¹⁶.

RNA-seq and transcriptome analysis (protocol used by the Xue laboratory). Total RNA was extracted from PD-1⁺CXCR5⁺ cells sorted from *Tcf7^{-/-}Lef1^{-/-}* mice or their control littermates, and two samples were obtained for each genotype. cDNA synthesis and amplification were performed with a SMARTer Ultra Low Input RNA Kit, starting with 10 ng of total RNA per sample, according to the manufacturer's instructions (Clontech). cDNA was fragmented with a Q800R sonicator (Qsonica) and was used as input for a NEBNext Ultra DNA Library Preparation Kit (NEB). Libraries were sequenced on a HiSeq2000 (Illumina) in single-read mode, with a read length of 50 nucleotides producing 60×10^6 to 70×10^6 reads per sample. Sequence data in ‘fastq’ format were generated with the CASAVA 1.8.2 processing pipeline from Illumina.

The sequencing quality of RNA-seq libraries was assessed by the FastQC quality control tool for high-throughput sequence data (version 0.10.1; Bioinformatics Group of the Babraham Institute). Because of biased GC content in the 5' end, the first 12 bases of each read in all four samples were ‘trimmed off’. The reproducibility of RNA-seq data was evaluated by computation of Pearson's correlation of FPKM (fragments per kilobase of exon per million fragments mapped) values for all genes in biological replicates. The Pearson's correlation coefficient between the two biological replicates was 0.937 for the control samples and 0.986 for the *Tcf7^{-/-}Lef1^{-/-}* samples, indicative of good reproducibility.

The RNA-seq libraries were then processed by the RSEM package (‘RNA-seq by Expectation-Maximization’; version 1.2.19) for estimation of the expression level of each gene. The expression level of a gene is reported as a ‘gene-level’ FPKM value. EBSeq (version 1.5.4), an integral component of the RSEM package, was used for the identification of differentially expressed genes. Genes of the mm9 (UCSC) assembly of the mouse genome from the iGenome collection of reference sequences were used for gene annotation.

RNA-seq and transcriptome analysis (protocol used by the Crotty laboratory). Cells were stored in Trizol, and total RNA was extracted from the cells with an miRNeasy Mini Kit (Qiagen 217004). For RNA-seq analysis of early

T_{FH} cells and T_{H1} cells: poly(A) RNA was isolated from 200 ng total RNA of each sample through the use of a Poly(A) Purist MAG kit (AM1922; Ambion). The resulting poly(A) RNA was then fragmented and prepared according to the manufacturer's instructions (ABI 4452437 Rev B), into 'bar-coded', strand-specific libraries with The SOLiD Total RNA-seq Kit (ABI 4445374). Following library preparation, 15 ng of each library was converted into SOLiD Wildfire compatible fragments with a 5500 W Conversion Primer Kit (Life Technologies) and five rounds of PCR. Libraries were then pooled at equimolar concentrations with a Quant-iT PicoGreen dsDNA Assay Kit (Life Technologies) and were sequenced on a 5500XL W Genetic Analyzer (Life Technologies). SOLiD 5500-2 sequencing outcomes were converted from 'color space' to 'nucleotide space' through the use of solid2fastq script (Galaxy). For RNA-seq analysis of GFP-RV⁺ or *Lef1*-RV⁺ SMARTA cells obtained 4 d after infection with LCMV, 500 ng of each sample's total RNA was prepared into mRNA libraries according to manufacturer's instructions (RS-122-2103; Illumina). The resulting libraries were deep sequenced on an Illumina 2500 in Rapid Run Mode, through the use of single-end reads with a length of 50 nucleotides (>24 × 10⁶ reads per condition). The single-end reads that passed Illumina filters were filtered for reads aligning to tRNA, rRNA, adaptor sequences, and 'spike-in' controls.

The reads were then aligned to the UCSC mm9 reference genome through the use of TopHat software (version 1.4.1). 'DUST scores' (for filtering low-complexity regions) were calculated with PRINSEQ Lite data preprocessing software (version 0.20.3), and low-complexity reads (with a 'DUST score' of >4) were removed from the BAM files (binary alignment map). The alignment results were parsed via SAMtools to generate SAM files (sequence alignment map). Read counts to each genomic feature were obtained with the htseq-count program (version 0.6.0) with the 'union' option. After removal of absent features (zero counts in all samples), the raw counts were then imported to software of the R project for statistical computing (R/Bioconductor package DESeq2) for the identification of genes differentially expressed among samples. DESeq2 normalizes counts by dividing each column of the 'count table' (samples) by the size factor of the column. The size factor is calculated by division of the samples by geometric means of the sequence reads of the genes. This brings the count values to a common scale suitable for comparison. *P* values for differential expression were calculated with the binomial test for differences between the base means of two conditions. These *P* values were then adjusted for multiple-test correction with the Benjamini-Hochberg algorithm to control the false-discovery rate. We considered genes as being expressed differentially between two groups of samples when the DESeq2 analysis resulted in an adjusted *P* value of <0.05 and the difference in gene expression was 1.5-fold. Cluster analyses, including principal-component analysis and hierarchical

clustering, were performed with standard algorithms and metrics. Hierarchical clustering was performed with complete linkage with Euclidean metric.

Heat maps. Heat maps were generated with normalized data of RNA-seq analyses for early T_{FH} cells and T_{H1} cells and for GFP-RV⁺ and *Lef1*-RV⁺ T_{FH} cells and T_{H1} cells. Microarray analysis used published T_{H1} cell sets, T_{FH} cell sets and GC T_{FH} cell sets (GEO accession code [GSE21380](#))⁵¹ and the GenePattern software suite (Broad Institute).

GSEA. GSEA was performed with GSEA software from the Broad Institute. Gene sets were generated in-house with genes that had a difference in expression of more than twofold in T_{FH} cells (PD-1^{lo}CXCR5⁺) and GC T_{FH} cells (PD-1^{hi}CXCR5⁺) relative to their expression in T_{H1} cells (PD-1⁻CXCR5⁻) (GEO accession code [GSE21380](#)). Enrichment for genes that were upregulated more than 1.2-fold in *Lef1*-RV⁺ T_{H1} cells relative to their expression in GFP-RV⁺ T_{H1} cells was then ranked by the 'Diff_of_Classes' metric of GSEA software.

ChIP. Sorted CD4⁺ T cells were cross-linked for 5 min with 1% formaldehyde in medium, were processed with a truChIP Chromatin Shearing Reagent Kit (Covaris) and were sonicated for 5 min on Covaris S2 ultrasonicator. The sheared chromatin was immunoprecipitated with anti-TCF-1 (C46C7; Cell Signaling Technologies) or control rabbit immunoglobulin G (2729; Cell Signaling Technologies) and was washed as described¹⁸. The immunoprecipitated DNA segments were used for quantification by PCR. For calculation of enrichment in the binding of TCF-1 in a given cell type, each ChIP sample analyzed with TCF-1 was first normalized to corresponding ChIP sample analyzed with immunoglobulin G, and the signal at a target region was then normalized to that at the *Hprt* promoter region.

Statistical analysis. Data sets were analyzed with the Student's *t*-test with a two-tailed distribution assuming equal sample variance.

48. Oxenius, A., Bachmann, M.F., Zinkernagel, R.M. & Hengartner, H. Virus-specific MHC-class II-restricted TCR-transgenic mice: effects on humoral and cellular immune responses after viral infection. *Eur. J. Immunol.* **28**, 390–400 (1998).
49. Kaji, T. *et al.* Distinct cellular pathways select germline-encoded and somatically mutated antibodies into immunological memory. *J. Exp. Med.* **209**, 2079–2097 (2012).
50. Choi, Y.S. & Crotty, S. Retroviral vector expression in TCR transgenic CD4⁺ T cells. *Methods Mol. Biol.* **1291**, 49–61 (2015).
51. Yusuf, I. *et al.* Germinal center T follicular helper cell IL-4 production is dependent on signaling lymphocytic activation molecule receptor (CD150). *J. Immunol.* **185**, 190–202 (2010).